

**MS amt-2018-230, Kunert et al.: Twin-plate ice nucleation assay (TINA) with infrared detection for high-throughput droplet freezing experiments with biological ice nuclei in laboratory and field samples**

We thank referee #1 for his comments, questions, and suggestions, which are highly appreciated and have been taken into account upon revision of our manuscript. The comments and our answers are listed below.

**Referee comment: The authors should stress what is the scientific innovation in their instrument given the very recent paper of Harrison et al. (2018), which was mentioned shortly in the end of the introduction section.**

Author's response: TINA studies ice nucleation in 960 microliter range droplets in one experiment, which enables the analysis of many samples or dilution series with good statistics in a short period of time. The cooling system allows a fast and high-precision temperature control over a wide temperature range at variable cooling rates. The infrared detection is an efficient method to doubtlessly determine freezing events, which was first applied to droplet freezing assays by Zaragotas et al. 2016. As discussed by Grothe 2018 (doi:10.5194/amt-2018-177-RC3, 2018), the authors of Harrison et al. 2018 attended several workshops and conferences and also have been the organizers for one conference, where our Twin-plate ice nucleation assay (TINA) with infrared detection was presented and discussed, so that our new setup was well-known to them.

**Referee comment: Also, why infrared detector enables improved detection over other methods?**

Author's response: The infrared detector monitors the temperature of each droplet during cooling. As soon as a droplet freezes, latent heat is released and a sharp signal can be detected. For clarification, we modified the last sentence of paragraph 2 in section 1, where we replaced "improved" by "efficient".

**Referee comment: The ability of high-throughput experiments was mentioned repeatedly in the manuscript, and it will be valuable contribution if the authors could use their existing data to show if this ability is important.**

Author's response: TINA is suitable for high-throughput experiments because the instrument enables the study of ice nucleation in 960 microliter range droplets in one experiment, which enables the analysis of many samples or dilution series with good statistics in a short period of time. This is demonstrated in Figure 10, for which aqueous extracts of two aliquots of an atmospheric aerosol filter sample were treated in three different ways. All treated samples and untreated controls were measured in five different dilutions to provide the full ice nucleation spectrum for each sample. Each dilution was measured in 96 droplets, and every sample consisted of two aliquots. All in all, 4608 droplets were measured for Figure 10, which correspond to six experiments performed by TINA. For each freezing experiment down to -30 °C, TINA takes about 45 min, which means 4.5 h of operation of TINA for Figure 10.

**Referee comment: I also wonder why error bars are lacking from all data and figures.**

Author's response: The uncertainty of the temperature sensor was used as the error of the temperature and was added into the figure captions. The error of the IN number concentrations was calculated using the counting error and the Gaussian error propagation, and error bars of the IN number concentrations were added into all figures.

The section 2.4 was optimized and the following paragraph was included:

“Assuming ice nucleation as a time-independent (singular) process, the number concentration of IN ( $\frac{\Delta N_m}{\Delta T}$ ) active at a certain temperature ( $T$ ) per unit mass of material is given by Eq. (1) (Vali, 1971a).

$$\frac{\Delta N_m}{\Delta T}(T) = -\ln\left(1 - \frac{s}{a - \sum_{i=0}^j s}\right) \cdot \frac{c}{\Delta T} \quad ; 0 \leq j \leq a \quad (1)$$

$$\text{with } c = \frac{V_{\text{wash}}}{V_{\text{drop}}} \cdot \frac{d}{m} \quad (2)$$

where  $s$  is the number of freezing events in 0.1 K bins ( $\Delta T$ ),  $a$  is the number of all droplets,  $m$  is the mass of the particles in the initial suspension,  $V_{\text{wash}}$  is the volume of the initial suspension,  $V_{\text{drop}}$  is the droplet volume, and  $d$  is the dilution factor of the droplets relative to  $m$ . The measurement uncertainty ( $\delta \frac{\Delta N_m}{\Delta T}(T)$ ) was calculated using the counting error of  $s$  plus one digit and the Gaussian error propagation (Eq. (3)).

$$\delta \frac{\Delta N_m}{\Delta T}(T) = \sqrt{\left(\frac{1}{1 - \frac{s}{a - \sum_{i=0}^j s}} \cdot \frac{c}{\Delta T} \cdot \frac{\sqrt{s+1}}{a - \sum_{i=0}^j s}\right)^2 + \left(\frac{1}{1 - \frac{s}{a - \sum_{i=0}^j s}} \cdot \frac{c}{\Delta T} \cdot \frac{s \cdot \sqrt{\sum_{i=0}^j s + 1}}{(a - \sum_{i=0}^j s)^2}\right)^2} \quad (3)$$

The cumulative IN number concentration ( $N_m(T)$ ) is given by Eq. (4).

$$N_m(T) = -\ln\left(1 - \frac{\sum_{i=0}^j s}{a}\right) \cdot c \quad ; 0 \leq j \leq a \quad (4)$$

The error of the cumulative IN number concentration ( $\delta N_m(T)$ ) was calculated using Eq. (5).

$$\delta N_m(T) = \sqrt{\left(\frac{c}{1 - \frac{\sum_{i=0}^j s}{a}} \cdot \frac{\sqrt{\sum_{i=0}^j s + 1}}{a}\right)^2} \quad (5)$$

According to the above equations, the uncertainty is proportional to the number of frozen droplets per temperature bin. In the freezing experiments described below, the lowest number of freezing events and largest uncertainties were obtained at the lower and higher end of each dilution series (Poisson distribution). Data points with uncertainties  $\geq 100\%$  were excluded (overall less than 6% of the measurement data).”

Specific comments:

**Referee comment: Line #26: It is stated that there is a good agreement with literature data. Where was this shown or detailed in the manuscript?**

**Author’s response:** In section 3.2, we discussed the results of our experiments with Snomax<sup>®</sup>, which are shown in Figures 7 and S4. “These findings are in accordance with the results of Budke and Koop (2015).” Here, we replaced “in accordance” with “in good agreement”.

In the same section, we also discussed the results of our experiments with *Mortierella alpina*, which are shown in Figures 8 and S5. “The cumulative number of IN and the initial freezing temperature of 268 K (-5 °C) are in good agreement with the literature (Fröhlich-Nowoisky et al., 2015; Pummer et al., 2015).”

**Referee comment: Line #76: I think it is confusing: up to 10 K min<sup>-1</sup> or more?**

**Author’s response:** We tested our setup with continuous cooling rates of up to 10 K min<sup>-1</sup>, but it is possible to run the setup at higher cooling rates. But it has to be considered, that for each cooling rate a new correction matrix has to be generated. For clarification, we deleted “or more”.

Referee comment: Line #83: Is this the correct place to introduce the similar approach by Harrison et al.?

Author's response: We deleted the sentence "Very recently, a similar approach for droplet freezing experiments with IR detection has been presented by Harrison et al. (2018), investigating K-feldspar, NX-illite, and atmospheric aerosol samples." at the end of section 1, and we modified in section 1: "Infrared (IR) detectors enable efficient detection of droplet freezing (Harrison et al., 2018; Zaragotas et al., 2016)."

Referee comment: Line #94: Here it is not clear if the plates are commercial product or self-designed? If commercial, manufacture details should be specified.

Author's response: We added the following sentence: "For each experiment, new sterile multiwell plates are used (96-well: Axon Labortechnik Kaiserslautern, Germany, 384-well: Eppendorf, Hamburg, Germany)."

Referee comment: Line #137: It confused me that it was cooled to 218.2 K and heated from 220.7 K?

Author's response: To clarify this, we modified the sentence: "The temperature within the bath was cooled down from 303.2 K to 218.2 K (30.0 °C to -55.0 °C) in 5 K steps, warmed to 220.7 K (-52.5 °C), and raised again from 220.7 K to 300.7 K (-52.5 °C to 27.5 °C) in 5 K steps."

Referee comment: Section 2.2: So what is the temperature uncertainty of TINA and how was it propagated?

Author's response: The temperature uncertainty of TINA is 0.2 K. We added the following sentence at the end of section 2.2: "From the calibration measurements, we obtained a total uncertainty estimate of  $\delta_{\text{total}} < 0.2$  K ( $\delta_{\text{total}} = \delta_{\text{Thermistor}} + \delta_{\text{TC}} + \delta_{\text{Morti}}$ )."

Referee comment: Line 144: I think it is still not clear at this point what is the temperature gradient you refer to. I would first defined that.

Author's response: We included thermocouple measurements in the individual wells of the sample holder blocks to correct for a temperature gradient within the two blocks. We added the following paragraph at the end of section 2.2. and included four new figures (Figure 4, S1, S2, S3) while renaming the existing. "To determine a potential temperature gradient of the sample holder blocks, two thermocouples (K type, 0.08 mm diameter, Omega) were positioned in various wells of multiwell plates (Figure S1a/b), each filled with 30  $\mu$ L pure water (see Sect. 3.1). These thermocouples were connected to the thermocouple in the elevation of each sample holder block, and the temperature offset between sample holder block and wells was measured for a continuous cooling rate of 1 K min<sup>-1</sup> (Figure S1c). Below -2 °C, the temperature offset between sample holder block and wells is nearly constant, in this example ~0.16 K and ~0.19 K. The measurement was performed in duplicates for all observed wells. Figure S2 shows the temperature gradient exemplarily for the 384-well sample holder block in a 2D interpolation based on all measurements.

To characterize the uncertainty of this measurement, the two thermocouples were placed in an ice water bath, and the sample holder block was cooled down to 2 °C, 1 °C, 0 °C, -1 °C, and -2 °C ( $T_{\text{block}}$ ), while the difference between the ice water and the block temperature was monitored by the thermocouples ( $T_{\text{diffTC}}$ ) (Figure S3). From these experiments, we obtained thermocouple uncertainties  $\delta_{\text{TC}} < 0.05$  K ( $\delta_{\text{TC}} = T_{\text{block}} + T_{\text{diffTC}}$ ).

Additionally, we used undiluted IN filtrate of *Mortierella alpina* 13A (see Sect. 3.2) as calibration substance, and a freezing experiment was performed as described for the biological reference materials (see Sect. 3.2). These results were used to compensate for the temperature

gradient, and the thermocouple measurements were used to correct the temperature offset between gradient-corrected wells and thermistors. A correction matrix was calculated, and this matrix was used to correct subsequent freezing experiments. Figure 4 shows the results of the fungal IN filtrate measurement (a) before and (b) after correction. After correction, all fungal IN filtrate measurements showed a standard deviation of  $< 0.06$  K ( $\delta_{\text{Morti}}$ ). From the calibration measurements, we obtained a total uncertainty estimate of  $\delta_{\text{total}} < 0.2$  K ( $\delta_{\text{total}} = \delta_{\text{Thermistor}} + \delta_{\text{TC}} + \delta_{\text{Morti}}$ )."

Referee comment: Line #151: please clarify why do you mention here Zaragotas et al. (2016).

Author's response: We deleted the sentence "In contrast, Zaragotas et al. (2016) used infrared camera, which was calibrated only once by the company, to measure the accurate temperature of each droplet."

Referee comment: Line #152: I think it would be nice if you will add the plate temperature at the different images.

Author's response: We thank the referee for this suggestion, and we added the plate temperature at the different images.

Referee comment: Line #157: what is the resolution in which images are taken?

Author's response: We added the information about the resolution of the images to section 2.3 to specify the method: "The camera has a resolution of 206 x 156 pixels, and it takes ten pictures per second. These pictures are averaged to one picture per second."

Referee comment: Line #182: Are those new plates? or the same plates described earlier in the text?

Author's response: We changed the sentence as follows: "For background measurements, 3  $\mu$ L aliquots of autoclaved and filtered pure water were pipetted into new sterile multiwell plates by a liquid handling station."

Moreover, we added this information in section 2.1.: "For each experiment, new sterile multiwell plates are used (96-well: Axon Labortechnik Kaiserslautern, Germany, 384-well: Eppendorf, Hamburg, Germany)."

Referee comment: Line #209: Please add a reference to this claim.

Author's response: We assume that different plates from different manufactures can lead to differences in freezing because of the production process and well shape, but cannot add a specific reference. For clarification we changed the sentence as follows: "The 96-well plates were obtained from a different manufacturer than the 384-well plates."

Referee comment: Line #235: Is this correct? Class A only seen for high suspension concentrations.

Author's response: We thank the referee for this comment. We removed the following text: "These differences result from three different classes of IN with different activation temperatures as described by Turner et al. (1990). Based on this classification, the Snomax<sup>®</sup> sample contains a large number of class A and C IN, but only a few IN of class B. These findings are in accordance with the results of Budke and Koop (2015). Below 259 K (-14 °C), a flat plateau arises where no IN are active." and we included the following sentence: "These findings are in good agreement with the results of Budke and Koop (2015)"

Referee comment: Line #302: per liter air? Or liter water.



189 Author's response: The IN concentration was calculated per liter air, which passed the filter  
190 during sampling. We included the following sentence: "All IN concentrations were calculated  
191 per liter air."

192  
193

194 Technical corrections:

195

196 Referee comment: Line #97: Fig. 1b should be describes before Fig. 1c.

197 Author's response: Changed as suggested.

198

199 Referee comment: Line #165: add "is" after Vdrop, and m, and etc..

200 Author's response: We modified the sentence.

201

202 Referee comment: Line #206: You can remove 'respectively'.

203 Author's response: This has been removed.

204

205 Referee comment: Line #209: 'showed' and not 'show'. Also found in other places in the text.

206 Author's response: We replaced it in several places in the text.

**MS amt-2018-230, Kunert et al.: Twin-plate ice nucleation assay (TINA) with infrared detection for high-throughput droplet freezing experiments with biological ice nuclei in laboratory and field samples**

We thank referee #2 for his comments, questions, and suggestions, which are highly appreciated and have been taken into account upon revision of our manuscript. The comments and our responses are listed below.

Referee comment 1: Line 21, please be clear what does “deviations  $<0.5$  K” mean and why it is high-precision temperature control.

Author’s response: We recalculated our maximum total error and replaced “deviations  $< 0.5$  K” by “uncertainty  $< 0.2$  K”. We included a new Figure S3, which shows the high-precision temperature control, by which TINA is operated.

Referee comment 2: Line 37, it is not clear why this method is suitable for high-throughput experiments and efficient analysis for field samples. I guess the authors don’t mean in-situ field measurement? If I understood it right, as for the demonstration of the field sample in the manuscript, one should collect enough sample and extract them carefully to get different dilutions for nm(T) measurements.

Author’s response: TINA is suitable for high-throughput experiments because the instrument enables the study of ice nucleation in 960 microliter range droplets in one experiment, which enables the analysis of many samples or dilution series with good statistics in a short period of time. This is demonstrated in Figure 10, for which aqueous extracts of two aliquots of an atmospheric aerosol filter sample were treated in three different ways. All treated samples and untreated controls were measured in six different dilutions to provide the full ice nucleation spectrum for each sample. Each dilution was measured in 96 droplets. All in all, 4608 droplets were measured for Figure 10, which correspond to six experiments performed by TINA. For each freezing experiment down to  $-30$  °C, TINA takes about 45 min, which means 4.5 h of operation of TINA for Figure 10.

Referee comment 3: Line 52-53, why the IR detector is better for droplet freezing detection? Please provide more details.

Author’s response: The infrared camera monitors the temperature of each droplet during cooling. As soon as a droplet freezes, latent heat is released and a sharp signal can be detected. We modified the last sentence of paragraph 2 in section 1, where we replaced “improved” by “efficient”.

Referee comment 4: Line 79-80, the two biological INPs are very efficient IN, TINA could work very well with such efficient INPs. How about the situation when the unknown samples are less efficient especially when background freezing start contribute the freezing at e.g.,  $-26$  °C or higher.

Author’s response: Our experiments with aqueous extracts of atmospheric aerosols confirm that TINA is suitable for freezing experiments of samples with unknown IN in a temperature range down to  $-25$  °C. Below this temperature, background freezing needs to be considered.

Referee comment 5: Line 140, how the droplet temp. is calibrated? you only calibrate the sensors as described? Line 150, the sample temperature needs to be calibrated., not just the sensor. Where are the thermistors in the experimental setup? Depending the location, likely there will be thermal lag due to the plate thickness and different cooling rate. And is the temp. uniform cross such large sample plate? This could also contribute to the different freezing curves for different plates (or plate designs).

Author's response: We included thermocouple measurements in the individual wells of the sample holder blocks to correct for a temperature gradient within the two blocks. We added the following paragraph at the end of section 2.2. and included four new figures (Figure 4, S1, S2, S3) while renaming the existing. "To determine a potential temperature gradient of the sample holder blocks, two thermocouples (K type, 0.08 mm diameter, Omega) were positioned in various wells of multiwell plates (Figure S1a/b), each filled with 30  $\mu$ L pure water (see Sect. 3.1). These thermocouples were connected to the thermocouple in the elevation of each sample holder block, and the temperature offset between sample holder block and wells was measured for a continuous cooling rate of 1 K min<sup>-1</sup> (Figure S1c). Below -2 °C, the temperature offset between sample holder block and wells is nearly constant, in this example ~0.16 K and ~0.19 K. The measurement was performed in duplicates for all observed wells. Figure S2 shows the temperature gradient exemplarily for the 384-well sample holder block in a 2D interpolation based on all measurements.

To characterize the uncertainty of this measurement, the two thermocouples were placed in an ice water bath, and the sample holder block was cooled down to 2 °C, 1 °C, 0 °C, -1 °C, and -2 °C ( $T_{\text{block}}$ ), while the difference between the ice water and the block temperature was monitored by the thermocouples ( $T_{\text{diffTC}}$ ) (Figure S3). From these experiments, we obtained thermocouple uncertainties  $\delta_{\text{TC}} < 0.05$  K ( $\delta_{\text{TC}} = T_{\text{block}} + T_{\text{diffTC}}$ ).

Additionally, we used undiluted IN filtrate of *Mortierella alpina* 13A (see Sect. 3.2) as calibration substance, and a freezing experiment was performed as described for the biological reference materials (see Sect. 3.2). These results were used to compensate for the temperature gradient, and the thermocouple measurements were used to correct the temperature offset between gradient-corrected wells and thermistors. A correction matrix was calculated, and this matrix was used to correct subsequent freezing experiments. Figure 4 shows the results of the fungal IN filtrate measurement (a) before and (b) after correction. After correction, all fungal IN filtrate measurements showed a standard deviation of  $< 0.06$  K ( $\delta_{\text{Morti}}$ ). From the calibration measurements, we obtained a total uncertainty estimate of  $\delta_{\text{total}} < 0.2$  K ( $\delta_{\text{total}} = \delta_{\text{Thermistor}} + \delta_{\text{TC}} + \delta_{\text{Morti}}$ )."

**Referee comment 6: Line 188, when using cooling rate of 1K/min, does the Wegener-Bergeron-Findeisen process affect the measurement?**

Author's response: The individual droplets are in separate compartments and do not influence each other during the freezing experiment.

**Referee comment 7: Line 256-257, please provide a brief description for the O3 and NO2 exposure experiment. Why such high concentration for both O3 and NO2 is used?**

Author's response: In section 3.3, we included the following paragraph: "Briefly, O<sub>3</sub> was produced by exposing synthetic air to UV light (L.O.T.-Oriol GmbH & Co. KG, Germany), and the O<sub>3</sub> concentration was adjusted by tuning the amount of UV light. The gas flow was ~1.9 L min<sup>-1</sup>, and it was mixed with N<sub>2</sub> containing ~5 ppmV NO<sub>2</sub> (Air Liquide, Germany). The NO<sub>2</sub> concentration was regulated by the addition of the amount of the ~5 ppmV NO<sub>2</sub> gas. The O<sub>3</sub> and NO<sub>2</sub> concentrations were monitored with commercial monitoring instruments (ozone analyzer: 49i, Thermo Scientific, Germany; NO<sub>x</sub> analyzer: 42i-TL, Thermo Scientific). The gas mixture was directly bubbled through 1 mL of the Snomax<sup>®</sup> solution at a flow rate of 60 mL min<sup>-1</sup> using a Teflon tube (ID: 1.59 mm). The Snomax<sup>®</sup> solution was exposed to a mixture of 1 ppm O<sub>3</sub> and 1 ppm NO<sub>2</sub> for 4 h, representing the exposure to an atmospherically relevant amount of about 200 ppb each for about 20 h. The exposure experiments were performed in triplicates. After exposure, the treated samples were serially diluted and the IN activity was measured as described for the Snomax<sup>®</sup> reference measurements."

Referee comment 8: Line 277, please provide the ice nucleation data for the field blank samples for comparison with ambient sample.

Author's response: We included the data for the blank sample in Figure 10.

Referee comment 9: Line 298-299, it is not clear why the decrease in IN activity after heat treatment is indication of the presence of biological IN.

Author's response: For clarification, we added the following sentence: "The concentration of IN active at temperatures above 263 K (-10 °C) was about 0.001 L<sup>-1</sup>, but heat treatment led to a loss of IN activity above 263 K (-10 °C). Because the activity of known biological IN results from proteins or proteinaceous compounds (Green and Warren, 1985; Kieft and Ruscetti, 1990; Pouleur et al., 1992; Tsumuki and Konno, 1994), and proteins are known to be heat-sensitive, the results suggest the presence of biological IN."

Referee comment 10: Line 307-314, it is suggested to carefully evaluate the discussion and conclusion in this section. As showing in Fig. 8, there is less than one order of magnitude different between the samples after 5  $\mu$ m and 0.1  $\mu$ m filtration. This could be just within measurement uncertainty, which is showing in Fig. S1 and S2, for each three independent samples that there is about one order of magnitude variation at certain temperature range.

Author's response: We thank the referee for his suggestion. We carefully evaluated the results and rewrote the paragraph: "Filtration experiments did not affect the initial freezing temperature, but the concentration of biological IN decreased significantly. The results suggest the presence of many biological IN or agglomerates larger than 5  $\mu$ m and of a few biological IN smaller than 0.1  $\mu$ m. The cumulative number of IN active between 263 K (-10 °C) and 257 K (-16 °C) decreased up to two orders of magnitude upon filtration, but the IN concentration below 256 K (-17 °C) was not affected. The findings show that many IN active between 263 K (-10 °C) and 257 K (-16 °C) were larger than 5  $\mu$ m, whereas IN active below 256 K (-17 °C) were smaller than 0.1  $\mu$ m."

Referee comment 11: Fig. 4, please provide the detail description for freezing determination using IR camera.

Author's response: The infrared camera monitors the temperature of each droplet during cooling. As soon as a droplet freezes, latent heat is released and a sharp signal can be detected. At the end of section 2.3, the freezing determination using IR camera is explained: "Software analysis uses a grid of 96 and 384 points, respectively, where the grid point is set to the center of each well enabling to fit the dimensions of each plate under different perspective angles. The temperature is tracked for each well during the experiment. A self-written algorithm detects a local maximum shortly followed by a local minimum in the derivative of the temperature profile, which is caused by the release of latent heat during freezing. The software exports the data for each droplet in CSV format."

Additionally, we added the information about the resolution of the images to section 2.3 to specify the method: "The camera has a resolution of 206 x 156 pixels, and it takes ten pictures per second. These pictures are averaged to one picture per second."

## List of changes

All changes have been marked in the revised version of the manuscript using track-changes. The most relevant changes are listed below.

### Author list:

The order was changed from “Anna T. Kunert<sup>1</sup>, Mark Lamneck<sup>2</sup>, Frank Helleis<sup>2</sup>, Mira L. Pöhlker<sup>1</sup>, Ulrich Pöschl<sup>1</sup>, and Janine Fröhlich-Nowoisky<sup>1,\*</sup>” to “Anna T. Kunert<sup>1</sup>, Mark Lamneck<sup>2</sup>, Frank Helleis<sup>2</sup>, Ulrich Pöschl<sup>1</sup>, Mira L. Pöhlker<sup>1,\*</sup>, and Janine Fröhlich-Nowoisky<sup>1,\*</sup>”

The following author was added to the corresponding authors:  
Mira L. Pöhlker

### Figures:

All figures of the manuscript and the supplementary material containing experimental data have been modified regarding data processing and error bars. Figure 4 was added to the manuscript. Figure 6a and 6b have been divided into two separate figures (Figure 7a and 8a), and differential IN spectra were added (Figure 7b and 8b). All subsequent figures have been renamed. In the supplementary material, the following figures have been added: S1, S2, S3, while renaming the existing.

### Section 2.2:

We included thermocouple measurements in the individual wells of the sample holder blocks to correct for a temperature gradient within the two blocks. We added the following paragraph at the end of section 2.2. and included four new figures (Figure 4, S1, S2, S3) while renaming the existing.

“To determine a potential temperature gradient of the sample holder blocks, two thermocouples (K type, 0.08 mm diameter, Omega) were positioned in various wells of multiwell plates (Figure S1a/b), each filled with 30  $\mu$ L pure water (see Sect. 3.1). These thermocouples were connected to the thermocouple in the elevation of each sample holder block, and the temperature offset between sample holder block and wells was measured for a continuous cooling rate of 1 K min<sup>-1</sup> (Figure S1c). Below -2 °C, the temperature offset between sample holder block and wells is nearly constant, in this example ~0.16 K and ~0.19 K. The measurement was performed in duplicates for all observed wells. Figure S2 shows the temperature gradient exemplarily for the 384-well sample holder block in a 2D interpolation based on all measurements.

To characterize the uncertainty of this measurement, the two thermocouples were placed in an ice water bath, and the sample holder block was cooled down to 2 °C, 1 °C, 0 °C, -1 °C, and -2 °C ( $T_{\text{block}}$ ), while the difference between the ice water and the block temperature was monitored by the thermocouples ( $T_{\text{diffTC}}$ ) (Figure S3). From these experiments, we obtained thermocouple uncertainties  $\delta_{\text{TC}} < 0.05$  K ( $\delta_{\text{TC}} = T_{\text{block}} + T_{\text{diffTC}}$ ).

Additionally, we used undiluted IN filtrate of *Mortierella alpina* 13A (see Sect. 3.2) as calibration substance, and a freezing experiment was performed as described for the biological reference materials (see Sect. 3.2). These results were used to compensate for the temperature gradient, and the thermocouple measurements were used to correct the temperature offset between gradient-corrected wells and thermistors. A correction matrix was calculated, and this



matrix was used to correct subsequent freezing experiments. Figure 4 shows the results of the fungal IN filtrate measurement (a) before and (b) after correction. After correction, all fungal IN filtrate measurements showed a standard deviation of  $< 0.06$  K ( $\delta_{\text{Morti}}$ ). From the calibration measurements, we obtained a total uncertainty estimate of  $\delta_{\text{total}} < 0.2$  K ( $\delta_{\text{total}} = \delta_{\text{Thermistor}} + \delta_{\text{TC}} + \delta_{\text{Morti}}$ )."

#### Section 2.4:

As requested by the referees, we included a detailed error calculation and added error bars to all figures. The error of the IN number concentrations was calculated using the counting error and the Gaussian error propagation. The total uncertainty estimate was used as the error of the temperature and was added into the figure captions. Additionally, we calculated the differential IN number concentration and plotted the corresponding spectrum.

The former section 2.4. was replaced by "Assuming ice nucleation as a time-independent (singular) process, the number concentration of IN ( $\frac{\Delta N_m}{\Delta T}$ ) active at a certain temperature ( $T$ ) per unit mass of material is given by Eq. (1) (Vali, 1971a).

$$\frac{\Delta N_m}{\Delta T}(T) = -\ln\left(1 - \frac{s}{a - \sum_{i=0}^j s}\right) \cdot \frac{c}{\Delta T} \quad ; 0 \leq j \leq a \quad (1)$$

$$\text{with } c = \frac{V_{\text{wash}}}{V_{\text{drop}}} \cdot \frac{d}{m} \quad (2)$$

where  $s$  is the number of freezing events in  $0.1$  K bins ( $\Delta T$ ),  $a$  is the number of all droplets,  $m$  is the mass of the particles in the initial suspension,  $V_{\text{wash}}$  is the volume of the initial suspension,  $V_{\text{drop}}$  is the droplet volume, and  $d$  is the dilution factor of the droplets relative to  $m$ . The measurement uncertainty ( $\delta \frac{\Delta N_m}{\Delta T}(T)$ ) was calculated using the counting error of  $s$  plus one digit and the Gaussian error propagation (Eq. (3)).

$$\delta \frac{\Delta N_m}{\Delta T}(T) = \sqrt{\left(\frac{1}{1 - \frac{s}{a - \sum_{i=0}^j s}} \cdot \frac{c}{\Delta T} \cdot \frac{\sqrt{s+1}}{a - \sum_{i=0}^j s}\right)^2 + \left(\frac{1}{1 - \frac{s}{a - \sum_{i=0}^j s}} \cdot \frac{c}{\Delta T} \cdot \frac{s \cdot \sqrt{\sum_{i=0}^j s+1}}{(a - \sum_{i=0}^j s)^2}\right)^2} \quad (3)$$

The cumulative IN number concentration ( $N_m(T)$ ) is given by Eq. (4).

$$N_m(T) = -\ln\left(1 - \frac{\sum_{i=0}^j s}{a}\right) \cdot c \quad ; 0 \leq j \leq a \quad (4)$$

The error of the cumulative IN number concentration ( $\delta N_m(T)$ ) was calculated using Eq. (5).

$$\delta N_m(T) = \sqrt{\left(\frac{c}{1 - \frac{\sum_{i=0}^j s}{a}} \cdot \frac{\sqrt{\sum_{i=0}^j s+1}}{a}\right)^2} \quad (5)$$

According to the above equations, the uncertainty is proportional to the number of frozen droplets per temperature bin. In the freezing experiments described below, the lowest number of freezing events and largest uncertainties were obtained at the lower and higher end of each dilution series (Poisson distribution). Data points with uncertainties  $\geq 100\%$  were excluded (overall less than 6% of the measurement data)."

#### Section 3.2:

We added additional differential IN spectra for the reference materials and rewrote the discussion:

“Three independent experiments with Snomax<sup>®</sup> showed reproducible results (Fig. S4), and, therefore, droplets of the same dilution were added to a total droplet number of 288. The obtained results were plotted in a cumulative and a differential IN spectrum (Fig. 7). The cumulative IN number concentration represents the total number of IN active above a certain temperature. The cumulative IN spectrum showed two strong increases, around 270 K (-3 °C) and around 265 K (-8 °C). These findings are in good agreement with the results of Budke and Koop (2015). The differential IN number concentration was calculated according to Vali (1971a), and it represents the number of IN active in a particular temperature interval. The differential IN spectrum showed a similar shape as the cumulative IN spectrum with a distinct plateau between 268 K and 266 K (-5 °C and -7 °C) and two slight maxima, around 269 K (-4 °C) and around 264 K (-9 °C). This indicates the presence of highly-efficient IN, active at a temperature of approximately 269 K (-4 °C), and less-efficient IN, active around 264 K (-9 °C). The fact that the less-efficient IN appeared in higher dilutions implies that they occur in higher concentrations than the highly-efficient IN. The presence of further IN with lower freezing temperatures and low concentrations cannot be excluded.”

“The cumulative and the differential IN spectra showed similar shapes with one maximum around 267 K (-6 °C), indicating the presence of one type of IN, which is highly-efficient.”

### Section 3.3:

We included the following paragraph to provide a brief description for the O<sub>3</sub> and NO<sub>2</sub> exposure experiments:

“Briefly, O<sub>3</sub> was produced by exposing synthetic air to UV light (L.O.T.-Oriel GmbH & Co. KG, Germany), and the O<sub>3</sub> concentration was adjusted by tuning the amount of UV light. The gas flow was ~1.9 L min<sup>-1</sup>, and it was mixed with N<sub>2</sub> containing ~5 ppmV NO<sub>2</sub> (Air Liquide, Germany). The NO<sub>2</sub> concentration was regulated by the addition of the amount of the ~5 ppmV NO<sub>2</sub> gas. The O<sub>3</sub> and NO<sub>2</sub> concentrations were monitored with commercial monitoring instruments (ozone analyzer: 49i, Thermo Scientific, Germany; NO<sub>x</sub> analyzer: 42i-TL, Thermo Scientific). The gas mixture was directly bubbled through 1 mL of the Snomax<sup>®</sup> solution at a flow rate of 60 mL min<sup>-1</sup> using a Teflon tube (ID: 1.59 mm). The Snomax<sup>®</sup> solution was exposed to a mixture of 1 ppm O<sub>3</sub> and 1 ppm NO<sub>2</sub> for 4 h, representing the exposure to an atmospherically relevant amount of about 200 ppb each for about 20 h. The exposure experiments were performed in triplicates. After exposure, the treated samples were serially diluted and the IN activity was measured as described for the Snomax<sup>®</sup> reference measurements.”

We rewrote the results:

“The results showed that gas exposure affected the IN activity of Snomax<sup>®</sup> (Fig. 9). High concentrations of O<sub>3</sub> and NO<sub>2</sub> reduced the cumulative number of IN from Snomax<sup>®</sup> between one and two orders of magnitude, while exposure to synthetic air showed smaller effects.”

### Section 3.4:

We carefully evaluated the results and rewrote the paragraph:

“Filtration experiments did not affect the initial freezing temperature, but the concentration of biological IN decreased significantly. The results suggest the presence of many biological IN or agglomerates larger than 5 µm and of a few biological IN smaller than 0.1 µm. The

cumulative number of IN active between 263 K (-10 °C) and 257 K (-16 °C) decreased up to two orders of magnitude upon filtration, but the IN concentration below 256 K (-17 °C) was not affected. The findings show that many IN active between 263 K (-10 °C) and 257 K (-16 °C) were larger than 5 µm, whereas IN active below 256 K (-17 °C) were smaller than 0.1 µm.”

We removed the following paragraph from the manuscript, because the outliers were excluded based on the introduced error calculation.

“The results of both, the untreated and the heated filter extracts, showed a few outliers. These were probably caused by single large particles or aggregates larger than 5 µm, which were statistically distributed over the different dilutions. These particles nucleated at warmer subfreezing temperatures than the other IN within a dilution, so they are overestimated due to their efficient nucleation. This hypothesis is supported by the fact that the filtered filter extracts did not contain any outliers.”

**Twin-plate ice nucleation assay (TINA) with infrared detection for high-throughput droplet freezing experiments with biological ice nuclei in laboratory and field samples**

Anna T. Kunert<sup>1</sup>, Mark Lamneck<sup>2</sup>, Frank Helleis<sup>2</sup>, Ulrich Pöschl<sup>1</sup>, Mira L. Pöhlker<sup>1,\*</sup> and Janine Fröhlich-Nowoisky<sup>1,\*</sup>

<sup>1</sup>Multiphase Chemistry Department, Max Planck Institute for Chemistry, 55128 Mainz, Germany

<sup>2</sup>Instrument Development and Electronics, Max Planck Institute for Chemistry, 55128 Mainz, Germany

*Correspondence to:* Janine Fröhlich-Nowoisky ([j.frohlich@mpic.de](mailto:j.frohlich@mpic.de)), Mira L. Pöhlker ([m.pohlker@mpic.de](mailto:m.pohlker@mpic.de))

Gelöscht: , Ulrich Pöschl<sup>1</sup>,

16 **Abstract.** For efficient analysis and characterization of biological ice nuclei under immersion  
 17 freezing conditions, we developed a Twin-plate Ice Nucleation Assay (TINA) for high-  
 18 throughput droplet freezing experiments, in which the temperature profile and freezing of each  
 19 droplet is tracked by an infrared detector. In the fully automated setup, a couple of  
 20 independently cooled aluminum blocks carrying two 96-well plates and two 384-well plates,  
 21 respectively, are available to study ice nucleation and freezing events simultaneously in  
 22 hundreds of microliter range droplets (0.1–40  $\mu\text{L}$ ). A cooling system with two refrigerant  
 23 circulation loops is used for high-precision temperature control (uncertainty  $< 0.2$  K), enabling  
 24 measurements over a wide range of temperatures ( $\sim 272$ – $233$  K) at variable cooling rates (up to  
 25  $10\text{ K min}^{-1}$ ).

26 The TINA instrument was tested and characterized in experiments with bacterial and  
 27 fungal ice nuclei (IN) from *Pseudomonas syringae* (Snomax<sup>®</sup>) and *Mortierella alpina*,  
 28 exhibiting freezing curves in good agreement with literature data. Moreover, TINA was applied  
 29 to investigate the influence of chemical processing on the activity of biological IN, in particular  
 30 the effects of oxidation and nitration reactions. Upon exposure of Snomax<sup>®</sup> to  $\text{O}_3$  and  $\text{NO}_2$ , the  
 31 cumulative number of IN active at 270–266 K decreased by more than one order of magnitude.  
 32 Furthermore, TINA was used to study aqueous extracts of atmospheric aerosols, simultaneously  
 33 investigating a multitude of samples that were pre-treated in different ways to distinguish  
 34 different kinds of IN. For example, heat treatment and filtration indicated that most biological  
 35 IN were larger than  $5\text{ }\mu\text{m}$ . The results confirm that TINA is suitable for high-throughput  
 36 experiments and efficient analysis of biological IN in laboratory and field samples.

Gelöscht: gradient

Gelöscht: deviations <

Gelöscht: 5

Gelöscht: -270

Gelöscht: and more

Gelöscht: samples

Gelöscht: concentration

Gelöscht: around 269

Gelöscht: ( $-4\text{ }^{\circ}\text{C}$ , “class A”)

Gelöscht: about two orders of magnitude, while the concentration of IN active around  $265\text{ K}$  ( $-8\text{ }^{\circ}\text{C}$ , “class C”) decreased by about

Gelöscht: experiments

Gelöscht: highly efficient

Gelöscht: smaller than  $0.1\text{ }\mu\text{m}$ , and many IN active between  $263\text{ K}$  ( $-10\text{ }^{\circ}\text{C}$ ) and  $256\text{ K}$  ( $-14\text{ }^{\circ}\text{C}$ ) were heat-resistant and



## 53 1 Introduction

54 Clouds and aerosols still contribute the largest uncertainty to the evaluation of the Earth's  
55 changing energy budget (Boucher et al., 2013). Thus, the understanding of the contribution of  
56 atmospheric aerosols in cloud processes is of fundamental importance. Atmospheric ice  
57 nucleation is essential for cloud glaciation and precipitation, thereby influencing the  
58 hydrological cycle and climate. Ice can be formed via homogeneous nucleation in liquid water  
59 droplets or heterogeneous nucleation triggered by particles serving as atmospheric ice nuclei  
60 (IN) (Pruppacher and Klett, 1997).

61 A wide range of droplet freezing assays and instruments have been developed and  
62 applied for the analysis of IN in immersion freezing experiments (e.g., Budke and Koop, 2015;  
63 Fröhlich-Nowoisky et al., 2015; Häusler et al., 2018; Murray et al., 2010; O'Sullivan et al.,  
64 2014; Stopelli et al., 2014; Tobo, 2016; Vali, 1971b; Whale et al., 2015; Wright and Petters,  
65 2013; Zaragotas et al., 2016). Most of the available assays and instruments, however, are limited  
66 to the investigation of small droplet numbers and use optical detection systems in the UV/Vis  
67 wavelength range.

68 Infrared (IR) detectors enable efficient detection of droplet freezing (Harrison et al.,  
69 2018; Zaragotas et al., 2016). Upon the phase change of water from liquid to solid, latent heat  
70 is released resulting in a sudden temperature change of the droplet, which can be detected by  
71 IR video thermography. In 1995, Ceccardi et al. (1995) used IR video thermography as a new  
72 technique to non-destructively study ice formation on plants by visualizing the changes in  
73 surface temperature. Wisniewski et al. (1997) evaluated the IR video thermography under  
74 controlled conditions and determined it as an excellent method for directly observing ice  
75 nucleation and propagation in plants. Since then, IR video thermography was used in a range  
76 of studies investigating freezing in plants (e.g., Ball et al., 2002; Carter et al., 1999; Charrier et  
77 al., 2017; Fuller and Wisniewski, 1998; Hacker and Neuner, 2007; Pearce and Fuller, 2001;  
78 Sekozawa et al., 2004; Stier et al., 2003; Wisniewski et al., 2008; Workmaster, 1999). Further  
79 applications of IR video thermography are investigations of cold thermal stress in insects  
80 (Gallego et al., 2016), monitoring of freeze drying processes (Emteborg et al., 2014), as well as  
81 detection of ice in wind turbine blades (Gómez Muñoz et al., 2016) and helicopter rotor blades  
82 (Hansman and Dershowitz, 1994). Freezing of single water droplets in an acoustic levitator has  
83 also been successfully observed by IR video thermography (Bauerecker et al., 2008).

84 Here, we introduce a Twin-plate Ice Nucleation Assay (TINA) for high-throughput  
85 droplet freezing experiments, in which the temperature profile and freezing of each droplet is  
86 tracked by an infrared detector. In the fully automated setup, a couple of independently cooled

**Gelöscht:** (e.g., Budke and Koop, 2015; Fröhlich-Nowoisky et al., 2015; Häusler et al., 2018; Murray et al., 2010; O'Sullivan et al., 2014; Stopelli et al., 2014; Tobo, 2016; Vali, 1971b, 1971a; Whale et al., 2015; Wright and Petters, 2013; Zaragotas et al., 2016). Most of the available assays and instruments, however, are limited to the investigation of small droplet numbers and use optical detection systems in the UV/Vis wavelength range. As shown by Zaragotas et al. (2016), however, infrared (IR) detector enable improved detection of droplet freezing.

**Gelöscht:** infrared (

**Gelöscht:** )

**Gelöscht:** gradient

aluminum blocks are available to study ice nucleation and freezing events in nearly 1000 microliter range droplets simultaneously. The instrument was developed in the course of the INUIT project over the last three years, in which it has been presented and discussed at several conferences and workshops (Kunert et al., 2016a, 2016b, 2017a, 2017b, 2018). We use the bacterial IN Snomax® and the IN-active fungus *Mortierella alpina* as biological test substances to investigate heterogeneous ice nucleation. Moreover, TINA is applied to investigate the effect of O<sub>3</sub> and NO<sub>2</sub> exposure on the IN activity of Snomax®. Furthermore, aqueous extracts of atmospheric aerosols are treated in different ways and are analyzed for different kinds of IN.

## 2 Experimental setup

### 2.1 Technical details

The core of the Twin-plate Ice Nucleation Assay (TINA) are two independently cooled, customized sample holder aluminum blocks, which have been shaped for multiwell plates with 96 and 384 wells, respectively. In each cooling block, two multiwell plates can be analyzed simultaneously. The maximal droplet volume in the 96-well block is 250 µL, and the minimal droplet volume is 0.1 µL, which is the limit of our liquid handling station (epMotion ep5073, Eppendorf, Hamburg, Germany). For each experiment, new sterile multiwell plates are used (96-well: Axon Labortechnik Kaiserslautern, Germany, 384-well: Eppendorf, Hamburg, Germany). As shown in Fig. 1, the design of the two sample holder blocks is basically identical, but the detailed construction varies slightly. Both blocks consist of two parts, a trough and a cap, which are screwed together and sealed with an O-ring. But, for the 96-well block (Fig. 1a), the cap is at the top (Fig. 1b), and the trough is at the bottom (Fig. 1c), whereas, for the 384-well block (Fig. 1d), the trough is at the top (Fig. 1e) and the cap is at the bottom (Fig. 1f). Two openings with Swagelok adapters for cooling liquid are placed next to each other, and the cooling liquid flows in a small passage around an elevation in the middle of the trough.

The customized sample holder blocks are cooled with a silicon-based cooling liquid (SilOil M80.055.03, Peter Huber Kältemaschinenbau AG, Offenburg, Germany) tempered by an external high-performance refrigeration bath circulator (CC-508 with Pilot ONE, Peter Huber Kältemaschinenbau AG), which can supply temperatures down to 218 K (-55 °C). Both sample holder blocks can be operated in parallel and independently from each other by use of two self-developed mixing valves and cooling loops (Fig. 2). This allows either the cooling of two different droplet freezing assays at the same time, or the observation of 960 droplets in one experiment. The mixing of a cold and a warm loop of cooling liquid for each block enables a fast and precise adjustment of the sample holder block temperatures without being dependent

**Gelöscht:** carrying two 96-well and two 384-well plastic plates, respectively,

**Gelöscht:** A cooling system with two refrigerant circulation loops is used for high-precision temperature control (deviations <0.5 K), enabling measurements over a wide range of temperatures (~233-270 K (~ -50 °C to -3 °C)) at variable cooling rates (up to 10 K min<sup>-1</sup> and more).

**Gelöscht:** Very recently, a similar approach for droplet freezing experiments with IR detection has been presented by Harrison et al. (2018), investigating K-feldspar, NX-illite, and atmospheric aerosol samples.

**Gelöscht:** ) and the cap is at the top (Fig. 1b

**Gelöscht:** due to the usage

147 on the cooling rate of the refrigeration bath circulator itself. In each experiment, the  
148 refrigeration bath circulator is cooled down 5 K below the coldest temperature, which is  
149 projected for the experiment, while no mixing of warm and cold cooling liquid occurs. By  
150 changing the position of the mixing valves for a defined period of time, cold and warm cooling  
151 liquids are mixed together, so that the desired temperatures within the two blocks are reached.  
152 Two pumps (VPP-655 PWM Single Version, Alphacool International GmbH, Braunschweig,  
153 Germany) ensure the continuous circulation of cooling liquid through each block independently  
154 from the position of the mixing valves. Figure 3 is a schematic illustration of the overall setup  
155 of TINA.

156

## 157 2.2 Temperature control and calibration

158 Within each sample holder block, the temperature is measured with two temperature sensors, a  
159 NTC thermistor in the cooling liquid stream (TH-44033, resistance: 2255  $\Omega$ /298 K,  
160 interchangeability:  $\pm 0.1$  K, Omega Engineering GmbH, Deckenpfronn, Germany) and a  
161 customized sensor with a NTC thermistor (10K3MRBD1, resistance: 10000  $\Omega$ /298 K,  
162 interchangeability:  $\pm 0.2$  K, TE Connectivity Company, Galway, Ireland) and a thermocouple  
163 (K type, 0.08 mm diameter, Omega), which were glued together in a 1/8 inch Swagelok® pipe,  
164 placed in the elevation. With further thermocouples connected to this reference, this offers the  
165 possibility to measure temperature differences between the NTC thermistor and arbitrary points  
166 simultaneously. Another NTC thermistor (10K3MRBD1, resistance: 10000  $\Omega$ /298 K,  
167 interchangeability:  $\pm 0.2$  K, TE Connectivity Company) monitors the temperature behind each  
168 mixing valve. Temperature control within the entire system is achieved by a self-developed  
169 microcontroller-based electronic system. The analog input unit is equipped with a 24 Bit Low  
170 Noise Delta-Sigma ADC (ADS1256), which assures the required accuracy to process the  
171 resolution of the used thermistors. All thermistors had been calibrated with a reference  
172 thermometer (2180A, Fluke Deutschland GmbH, Glottertal, Germany; 0.01 K resolution,  
173 system uncertainty  $\delta_{\text{Fluke}}$ :  $\pm 0.08$  K at 223 K and  $\pm 0.07$  K at 273 K). Therefore, all thermistors  
174 were bound together with a PT100 sensor of the reference thermometer, and the bundle was  
175 placed inside a brass cylinder filled with cooling liquid. The cylinder was placed inside the  
176 cooling bath of the refrigeration bath circulator. The temperature within the bath was cooled  
177 down from 303.2 K to 218.2 K (30.0 °C to -55.0 °C) in 5 K steps, warmed to 220.7 K (-  
178 52.5 °C), and raised again from 220.7 K to 300.7 K (-52.5 °C to 27.5 °C) in 5 K steps. Each  
179 step was kept for 30 min to equilibrate the temperature, while the resistance of all thermistors  
180 and the temperature measured by the reference thermometer were monitored. For the

Gelöscht: in the elevation.

Gelöscht: : 0.01 K, maximum

Gelöscht: error

Gelöscht: , Fluke Deutschland GmbH, Glottertal, Germany

conversion of the measured resistance of the thermistors into temperature, cubic spline interpolation was used ( $\delta_{\text{pol}} < 0.01 \text{ K}$ ). We obtained the thermistor calibration uncertainty  $\delta_{\text{Thermistor}} < 0.09 \text{ K}$  ( $\delta_{\text{Thermistor}} = \delta_{\text{Fluke}} + \delta_{\text{pol}}$ ).

To determine a potential temperature gradient of the sample holder blocks, two thermocouples (K type, 0.08 mm diameter, Omega) were positioned in various wells of multiwell plates (Figure S1a/b), each filled with 30  $\mu\text{L}$  pure water (see Sect. 3.1). These thermocouples were connected to the thermocouple in the elevation of each sample holder block, and the temperature offset between sample holder block and wells was measured for a continuous cooling rate of  $1 \text{ K min}^{-1}$  (Figure S1c). Below  $-2 \text{ }^{\circ}\text{C}$ , the temperature offset between sample holder block and wells is nearly constant, in this example  $\sim 0.16 \text{ K}$  and  $\sim 0.19 \text{ K}$ . The measurement was performed in duplicates for all observed wells. Figure S2 shows the temperature gradient exemplarily for the 384-well sample holder block in a 2D interpolation based on all measurements.

To characterize the uncertainty of this measurement, the two thermocouples were placed in an ice water bath, and the sample holder block was cooled down to  $2 \text{ }^{\circ}\text{C}$ ,  $1 \text{ }^{\circ}\text{C}$ ,  $0 \text{ }^{\circ}\text{C}$ ,  $-1 \text{ }^{\circ}\text{C}$ , and  $-2 \text{ }^{\circ}\text{C}$  ( $T_{\text{block}}$ ), while the difference between the ice water and the block temperature was monitored by the thermocouples ( $T_{\text{diffTC}}$ ) (Figure S3). From these experiments, we obtained thermocouple uncertainties  $\delta_{\text{TC}} < 0.05 \text{ K}$  ( $\delta_{\text{TC}} = T_{\text{block}} + T_{\text{diffTC}}$ ).

Additionally, we used undiluted IN filtrate of *Mortierella alpina* 13A (see Sect. 3.2) as calibration substance, and a freezing experiment was performed as described for the biological reference materials (see Sect. 3.2). These results were used to compensate for the temperature gradient, and the thermocouple measurements were used to correct the temperature offset between gradient-corrected wells and thermistors. A correction matrix was calculated, and this matrix was used to correct subsequent freezing experiments. Figure 4 shows the results of the fungal IN filtrate measurement (a) before and (b) after correction. After correction, all fungal IN filtrate measurements showed a standard deviation of  $< 0.06 \text{ K}$  ( $\delta_{\text{Morti}}$ ). From the calibration measurements, we obtained a total uncertainty estimate of  $\delta_{\text{total}} < 0.2 \text{ K}$  ( $\delta_{\text{total}} = \delta_{\text{Thermistor}} + \delta_{\text{TC}} + \delta_{\text{Morti}}$ ).

### 2.3 Infrared video thermography

Droplet freezing is determined by a distinct detection system, where the temperature profile of each single droplet is tracked by infrared cameras (Seek Thermal Compact XR, Seek Thermal Inc., Santa Barbara, CA, USA) coupled to a self-written software. The camera has a resolution of  $206 \times 156$  pixels, and it takes ten pictures per second. These pictures are averaged to one

Gelöscht: gradient

Gelöscht: This

picture per second. The concept enables a doubtless determination of freezing events because freezing of supercooled liquid releases energy, which leads to an abrupt rise in the detected temperature of the observed droplet, as discussed earlier (Sect. 1). This detection system uses the IR video thermography only to determine freezing events, while the proper temperature is monitored by thermistors. Figure 5 is a sequence of infrared camera images showing droplets during cooling and freezing (red circles). Software analysis uses a grid of 96 and 384 points, respectively, where the grid point is set to the center of each well enabling to fit the dimensions of each plate under different perspective angles. The temperature is tracked for each well during the experiment. A self-written algorithm detects a local maximum shortly followed by a local minimum in the derivative of the temperature profile, which is caused by the release of latent heat during freezing. The software exports the data for each droplet in CSV format.

## 2.4 Data analysis

Assuming ice nucleation as a time-independent (singular) process, the number concentration of IN ( $\frac{\Delta N_m}{\Delta T}$ ) active at a certain temperature ( $T$ ) per unit mass of material is given by Eq. (1) (Vali, 1971a).

$$\frac{\Delta N_m}{\Delta T}(T) = -\ln\left(1 - \frac{s}{a - \sum_{i=0}^j s}\right) \cdot \frac{c}{\Delta T}; 0 \leq j \leq a \quad (1)$$

$$\text{with } c = \frac{V_{\text{wash}}}{V_{\text{drop}}} \cdot \frac{d}{m} \quad (2)$$

where  $s$  is the number of freezing events in 0.1 K bins ( $\Delta T$ ),  $a$  is the number of all droplets,  $m$  is the mass of the particles in the initial suspension,  $V_{\text{wash}}$  is the volume of the initial suspension,  $V_{\text{drop}}$  is the droplet volume, and  $d$  is the dilution factor of the droplets relative to  $m$ . The measurement uncertainty ( $\delta \frac{\Delta N_m}{\Delta T}(T)$ ) was calculated using the counting error of  $s$  plus one digit and the Gaussian error propagation (Eq. (3)).

$$\delta \frac{\Delta N_m}{\Delta T}(T) = \sqrt{\left(\frac{1}{1 - \frac{s}{a - \sum_{i=0}^j s}} \cdot \frac{c}{\Delta T} \cdot \frac{\sqrt{s+1}}{a - \sum_{i=0}^j s}\right)^2 + \left(\frac{1}{1 - \frac{s}{a - \sum_{i=0}^j s}} \cdot \frac{c}{\Delta T} \cdot \frac{s \cdot \sqrt{\sum_{i=0}^j s + 1}}{(a - \sum_{i=0}^j s)^2}\right)^2} \quad (3)$$

The cumulative IN number concentration ( $N_m(T)$ ) is given by Eq. (4).

$$N_m(T) = -\ln\left(1 - \frac{\sum_{i=0}^j s}{a}\right) \cdot c; 0 \leq j \leq a \quad (4)$$

The error of the cumulative IN number concentration ( $\delta N_m(T)$ ) was calculated using Eq. (5).

**Gelöscht:** In contrast, Zaragotas et al. (2016) used infrared camera, which was calibrated only once by the company, to measure the accurate temperature of each droplet. Figure 4

**Gelöscht:** gradient

**Gelöscht:**  $n_m$

**Gelöscht:**  $n_m(T) = \frac{-\ln(1-f_{\text{ice}})}{V_{\text{drop}}} \cdot \frac{d}{m} \quad (1)$

**Gelöscht:**  $f_{\text{ice}}$

**Gelöscht:** fraction of frozen droplets at

**Gelöscht:** particular temperature,  $V_{\text{drop}}$

**Gelöscht:** droplet volume

**Gelöscht:** To simplify



$$\delta N_m(T) = \sqrt{\left( \frac{c}{1 - \frac{\sum_{i=0}^j s}{a}} \cdot \frac{\sqrt{\sum_{i=0}^j s+1}}{a} \right)^2} \quad (5)$$

According to the above equations, the uncertainty is proportional to the number of frozen droplets per temperature bin. In the freezing experiments described below, the lowest number of freezing events and largest uncertainties were obtained at the lower and higher end of each dilution series (Poisson distribution). Data points with uncertainties  $\geq 100\%$  were excluded (overall less than 6% of the measurement data).

**Gelöscht:** analysis, freezing events were merged in 0.1 K bins.

### 3. Freezing experiments

The fully automated TINA setup was tested and characterized for immersion freezing experiments with pure water droplets, as well as Snomax® and IN filtrate of the fungus *Mortierella alpina* as biological reference substances. Moreover, TINA was used to study the effect of O<sub>3</sub> and NO<sub>2</sub> exposure on the IN activity of Snomax®. Furthermore, TINA was applied to atmospheric aerosol samples.

#### 3.1 Pure water

Pure water was obtained from a Barnstead™ GenPure™ xCAD Plus water purification system (Thermo Scientific, Braunschweig, Germany). The water was autoclaved at 394 K (121 °C) for 20 min, filtered three times through a sterile 0.1 µm pore diameter sterile polyethersulfone (PES) vacuum filter unit (VWR International, Radnor, PA, USA), and autoclaved again.

For background measurements, 3 µL aliquots of autoclaved and filtered pure water were pipetted into new sterile multiwell plates by a liquid handling station. Therefore, four (96-well plate) and eight (384-well plate) different water samples were pipetted column-wise distributed into the plates. In total, six columns per sample were apportioned over the two twin-plates, i.e., 48 droplets per sample in 96-well plates, and 96 droplets per sample in 384-well plates. The plates were placed in the sample holder blocks and were cooled down quickly to 273 K (0 °C), and, as soon as the temperature was stable for one minute, in a continuous cooling rate of 1 K min<sup>-1</sup> further down to 238 K (-35 °C).

**Gelöscht:** 96-well

**Gelöscht:** (Axon Labortechnik, Kaiserslautern, Germany) and 384-well plates (Eppendorf), respectively,

As the phase transition from liquid water to ice is kinetically hindered, supercooled water can stay liquid at temperatures down to 235 K (-38 °C), where homogeneous ice nucleation takes place. This is only true for nanometer-sized droplets because the freezing temperature is dependent on droplet volume and cooling rate, and the classical nucleation theory predicts a homogeneous freezing temperature of about 240 K (-33 °C) for microliter

297 volume droplets using a cooling rate of 1 K min<sup>-1</sup> (Fornea et al., 2009; Murray et al., 2010;  
 298 Pruppacher and Klett, 1997; Tobo, 2016). However, several studies reported average freezing  
 299 temperatures for microliter volume droplets of pure water at significantly higher temperatures  
 300 because of possible artifacts (e.g., Conen et al., 2011; Fröhlich-Nowoisky et al., 2015; Hill et  
 301 al., 2016; Whale et al., 2015). To our knowledge, only two studies reported an average  
 302 homogeneous freezing temperature of 240 K (-33 °C) for microliter volume droplets and a  
 303 cooling rate of 1 K min<sup>-1</sup>, using hydrophobic surfaces as contact area for the droplets (Fornea  
 304 et al., 2009; Tobo, 2016). Providing microliter droplets free of suspended IN and surfaces free  
 305 of contaminants is difficult, so that the temperature limit below which freezing cannot be traced  
 306 back to heterogeneous IN needs to be determined individually for each setup.

307 Our results showed that most pure water droplets froze around 248 K (-25 °C) in 96-  
 308 well plates (Fig. 6a) and around 245 K (-28 °C) in 384-well plates (Fig. 6b). The 96-well plates  
 309 were obtained from a different manufacturer than the 384-well plates. All in all, these freezing  
 310 temperatures are substantially above the expected temperatures for homogeneous nucleation of  
 311 microliter droplets, but they are in accord with the results of Whale et al. (2015).

### 313 3.2 Biological reference materials

314 The performance of TINA was further assessed using Snomax® as a bacterial IN-active  
 315 reference substance (e.g., Budke and Koop, 2015; Hartmann et al., 2013; Möhler et al., 2008;  
 316 Turner et al., 1990; Ward and DeMott, 1989) and IN filtrate of the well-studied IN fungus  
 317 *Mortierella alpina* (Fröhlich-Nowoisky et al., 2015; Pummer et al., 2015).

318 Snomax® was obtained from SMI Snow Makers AG (Thun, Switzerland), and a stock  
 319 solution was prepared in pure water with an initial mass concentration of 1 mg mL<sup>-1</sup>. This  
 320 suspension was then serially diluted 10-fold with pure water by the liquid handling station. The  
 321 resulting Snomax® concentrations varied between 1 mg mL<sup>-1</sup> and 0.1 ng mL<sup>-1</sup>, equivalent to a  
 322 total mass of Snomax® between 3 µg and 0.3 pg, respectively, per 3 µL droplet.

323 Each dilution was pipetted column-wise distributed over the twin-plates as described  
 324 before in 96 droplets into 384-well plates by the liquid handling station. Two plates at a time  
 325 were placed inside the 384-well sample holder block, and the plates were cooled down quickly  
 326 to 273 K (0 °C), and, as soon as the temperature was stable for one minute, in a continuous  
 327 cooling rate of 1 K min<sup>-1</sup> further down to 253 K (-20 °C).

328 Three independent experiments with Snomax® showed reproducible results (Fig. S4),  
 329 and, therefore, droplets of the same dilution were added to a total droplet number of 288. The  
 330 obtained results were plotted in a cumulative and a differential IN spectrum (Fig. 7). The

Gelöscht: have

Gelöscht: warmer subfreezing

Gelöscht: due to

Gelöscht: show

Gelöscht: 247

Gelöscht: 26

Gelöscht: 244

Gelöscht: 29

[1] verschoben (Einfügung)

Gelöscht: 5a

Gelöscht: 5b), respectively. This discrepancy can have different explanations. First, the

Gelöscht: are

Gelöscht: Second, the different well shape leads to an altered shape of the droplet, which could influence its freezing abilities at very low temperatures.

Gelöscht: show reproducible results (Fig. S1). Therefore, droplets of the same dilution were added to a total droplet number of 288 (Fig. 6a). The data show two strong increases in the cumulative number of IN, one around 269 K (-4 °C) and one around 265 K (-8 °C), interrupted by a slightly increasing plateau between 268 K and 266 K (-5 °C and -7 °C). These differences result from three different classes of IN with different activation temperatures as described by Turner et al. (1990). Based on this classification, the Snomax® sample contains a large number of class A and C IN, but only a few IN of class B. These findings are in accordance

358 cumulative IN number concentration represents the total number of IN active above a certain  
 359 temperature. The cumulative IN spectrum showed two strong increases, around 270 K (-3 °C)  
 360 and around 265 K (-8 °C). These findings are in good agreement with the results of Budke and  
 361 Koop (2015). The differential IN number concentration was calculated according to Vali  
 362 (1971a), and it represents the number of IN active in a particular temperature interval. The  
 363 differential IN spectrum showed a similar shape as the cumulative IN spectrum with a distinct  
 364 plateau between 268 K and 266 K (-5 °C and -7 °C) and two slight maxima, around 269 K (-4  
 365 °C) and around 264 K (-9 °C). This indicates the presence of highly-efficient IN, active at a  
 366 temperature of approximately 269 K (-4 °C), and less-efficient IN, active around 264 K (-9 °C).  
 367 The fact that the less-efficient IN appeared in higher dilutions implies that they occur in higher  
 368 concentrations than the highly-efficient IN. The presence of further IN with lower freezing  
 369 temperatures and low concentrations cannot be excluded.

Gelöscht: Below 259 K (-14 °C), a flat plateau arises where no IN are active.

370 The analysis of different IN active within a wide temperature range was only possible  
 371 with the measurement of a dilution series. TINA enables the simultaneous measurement of such  
 372 a dilution series with high statistics in a short period of time.

Gelöscht: due to

373 *Mortierella alpina* 13A was grown on full-strength PDA (VWR International GmbH,  
 374 Darmstadt, Germany) at 277 K (4 °C) for 7 months. Fungal IN filtrate was prepared as described  
 375 previously (Fröhlich-Nowoisky et al., 2015; Pummer et al., 2015) and contained IN from spores  
 376 and mycelial surfaces. It was serially diluted 10-fold with pure water by the liquid handling  
 377 station. The experiment was performed as described above.

Gelöscht: 269

378 For test measurements with fungal IN, IN filtrate of three different culture plates from  
 379 *Mortierella alpina* 13A was measured, and the results were reproducible (Fig. S5). The  
 380 cumulative number of IN per gram mycelium only varied between one order of magnitude,  
 381 which is a good achievement for a biological sample, and droplets of the same dilutions were  
 382 added to a total droplet number of 288. A cumulative IN spectrum (Fig. 8a) and a differential  
 383 IN spectrum (Fig. 8b) were plotted. The cumulative number of IN and the initial freezing  
 384 temperature of 268 K (-5 °C) are in good agreement with the literature (Fröhlich-Nowoisky et  
 385 al., 2015; Pummer et al., 2015). The cumulative and the differential IN spectra showed similar  
 386 shapes with one maximum around 267 K (-6 °C), indicating the presence of one type of IN,  
 387 which is highly-efficient.

Gelöscht: S2

Gelöscht: varies

[1] nach oben verschoben: 6b).

Gelöscht: 267.7

Gelöscht: 5.

### 389 3.3 Ozonized and nitrated samples

To study the effect of O<sub>3</sub> and NO<sub>2</sub> exposure on the IN activity of Snomax<sup>®</sup>, an aliquot of 1 mL of a 1 mg mL<sup>-1</sup> suspension of Snomax<sup>®</sup> in pure water was exposed in liquid phase to gases with or without O<sub>3</sub> and NO<sub>2</sub> as described in Liu et al. (2017).<sup>▼</sup>

Briefly, O<sub>3</sub> was produced by exposing synthetic air to UV light (L.O.T.-Oriel GmbH & Co. KG, Germany), and the O<sub>3</sub> concentration was adjusted by tuning the amount of UV light. The gas flow was ~1.9 L min<sup>-1</sup>, and it was mixed with N<sub>2</sub> containing ~5 ppmV NO<sub>2</sub> (Air Liquide, Germany). The NO<sub>2</sub> concentration was regulated by the addition of the amount of the ~5 ppmV NO<sub>2</sub> gas. The O<sub>3</sub> and NO<sub>2</sub> concentrations were monitored with commercial monitoring instruments (ozone analyzer: 49i, Thermo Scientific, Germany; NO<sub>x</sub> analyzer: 42i-TL, Thermo Scientific). The gas mixture was directly bubbled through 1 mL of the Snomax<sup>®</sup> solution at a flow rate of 60 mL min<sup>-1</sup> using a Teflon tube (ID: 1.59 mm). The Snomax<sup>®</sup> solution was exposed to a mixture of 1 ppm O<sub>3</sub> and 1 ppm NO<sub>2</sub> for 4 h, representing the exposure to an atmospherically relevant amount of about 200 ppb each for about 20 h. The exposure experiments were performed in triplicates. After exposure, the treated samples were serially diluted and the IN activity was measured as described for the Snomax<sup>®</sup> reference measurements.

The results showed that gas exposure affected the IN activity of Snomax<sup>®</sup> (Fig. 9). High concentrations of O<sub>3</sub> and NO<sub>2</sub> reduced the cumulative number of IN from Snomax<sup>®</sup> between one and two orders of magnitude, while exposure to synthetic air showed smaller effects.

Snomax<sup>®</sup> contains IN proteins of the bacterium *Pseudomonas syringae*. Attard et al., (2012) found no significant or only weak effects of exposure to ~100 ppb O<sub>3</sub> and ~100 ppb NO<sub>2</sub> on the IN activity of two strains of *P. syringae*, and a variable response of a third strain, suggesting a strain-specific response.

### 3.4 Air filter samples

Total suspended particle samples were collected onto 150 mm glass fiber filters (Type MN 85/90, Macherey-Nagel GmbH, Düren, Germany) using a high-volume sampler (DHA-80, Digital Elektronik AG, Hegnau, Switzerland) operated at 1000 L min<sup>-1</sup>, which was placed at the roof of the Max Planck Institute for Chemistry (Mainz, Germany). There, a mix of urban and rural continental boundary layer air can be sampled in central Europe. The filter was taken in April 2018, and the sampling period was seven days, corresponding to a total air volume of approximately 10,000 m<sup>3</sup>. Filters were pre-baked at 603 K (330 °C) for 10 h to remove any biological material, and blank samples were taken to detect possible contaminations. All filters

**Gelöscht:** A dilution series of the treated samples was measured as described for the Snomax<sup>®</sup> reference measurements.

**Gelöscht:** The results show that high concentrations of O<sub>3</sub> and NO<sub>2</sub> reduce the concentration of IN active around 269 K (-4 °C, "class A") about two orders of magnitude, while the concentration of IN active around 265 K (-8 °C, "class C") decreased by about one order of magnitude (Fig. 7). The cumulative number of IN per unit mass is slightly reduced by the exposure to synthetic air, which can be explained by a small loss of IN within the system during exposure.

**Gelöscht:** MPIC,

444 were packed in pre-baked aluminum bags, and loaded filters were stored at 193 K (-80 °C) until  
445 analysis.

446 An aerosol and a blank filter were cut with a sterilized scissor into aliquots (~1/16), and  
447 the exact percentage was determined gravimetrically. For reproducibility, two filter sample  
448 aliquots of each filter were extracted. Each filter sample aliquot was transferred into a sterile  
449 50 mL tube (Greiner Bio One, Kremsmünster, Austria), and 10 mL of pure water was added.  
450 The tubes were shaken horizontally at 200 rpm for 15 min. Afterwards, the filter was removed,  
451 and the aqueous extract was tested for IN activity. To further characterize the IN, the effects of  
452 filtration and heat treatment were investigated. Therefore, aliquots of the extract were treated  
453 as follows: (i) 1 h at 371 K (98 °C), (ii) filtration through a 5 µm pore diameter filter (Acrodisc,  
454 PES, Pall, Germany), (iii) filtration through a 5 µm and a 0.1 µm pore diameter filter (Acrodisc).

455 Each solution (96 aliquots of 3 µL) was pipetted column-wise into 384-well plates by  
456 the liquid handling station. The plates were cooled down quickly to 273 K (0 °C), and, as soon  
457 as the temperature was stable for one minute, in a continuous cooling rate of 1 K min<sup>-1</sup> further  
458 down to 243 K (-30 °C).

459 Each solution of the two aliquots of each filter was measured separately, and droplets  
460 of the same solution were added to a total droplet number of 192 (2 x 96 droplets) (Fig. 10, S6).

461 All IN concentrations were calculated per liter air.

462 The untreated filter extract showed IN activity at relatively high temperatures with an  
463 initial freezing temperature of 267 K (-6 °C). The concentration of IN active at temperatures  
464 above 263 K (-10 °C) was about 0.001 L<sup>-1</sup>, but heat treatment led to a loss of IN activity above  
465 263 K (-10 °C). Because the activity of known biological IN results from proteins or  
466 proteinaceous compounds (Green and Warren, 1985; Kieft and Ruscetti, 1990; Pouleur et al.,  
467 1992; Tsumuki and Konno, 1994) and proteins are known to be heat-sensitive, the results  
468 suggest the presence of biological IN. The concentration of IN between 263 K (-10 °C) and 257  
469 K (-16 °C) increased about two orders of magnitude and in a sudden increase another two orders  
470 between 257 K (-16 °C) and 256 K (-17 °C). The IN concentration below 256 K (-17 °C)  
471 increased continuously up to about 500 L<sup>-1</sup>, but heat treatment reduced the IN concentration of  
472 up to one order of magnitude below 256 K (-17 °C). Filtration experiments did not affect the  
473 initial freezing temperature, but the concentration of biological IN decreased significantly. The  
474 results suggest the presence of many biological IN or agglomerates larger than 5 µm and of a  
475 few biological IN smaller than 0.1 µm. The cumulative number of IN active between 263 K (-  
476 10 °C) and 257 K (-16 °C) decreased up to two orders of magnitude upon filtration, but the IN  
477 concentration below 256 K (-17 °C) was not affected. The findings show that many IN active

Gelöscht: Filters

Gelöscht: aerosol and blank

Gelöscht: S3). For better clearness, data of different dilutions were averaged for each treatment (Fig. 8).

Gelöscht: warm subfreezing

Gelöscht: 10<sup>-3</sup>

Gelöscht: ), which indicates

Gelöscht: 255

Gelöscht: 18

Gelöscht: continuously

Gelöscht: 255

Gelöscht: 18

Gelöscht: 254

Gelöscht: 19

Gelöscht: A maximum

Gelöscht: of 10<sup>2</sup> L<sup>-1</sup> was reached around 250

Gelöscht: 23

Gelöscht: ),

Gelöscht: maximum

Gelöscht: 10<sup>1</sup> L<sup>-1</sup> at 250

Gelöscht: 23

Gelöscht: was

Gelöscht: about half an order of magnitude, at which

Gelöscht: 0.1

Gelöscht: filtration showed

Gelöscht: slightly bigger effect.

Gelöscht: concentration

Gelöscht: 256

Gelöscht: 17

Gelöscht: about

Gelöscht: 5 µm

Gelöscht: and 0.1 µm filtration reduced

Gelöscht: slightly more. The maximum IN concentration of 10<sup>2</sup> L<sup>-1</sup> around 250

Gelöscht: 23

Gelöscht: upon filtration. The results suggest that there were highly efficient biological IN smaller than 0.1 µm and other biological IN or agglomerates of the same biological IN with different sizes. Moreover, the



517 between 263 K (-10 °C) and 257 K (-16 °C) were larger than 5 µm, whereas IN active below  
518 256 K (-17 °C) were smaller than 0.1 µm.

Gelöscht: 256

Gelöscht: 17

Gelöscht: between

Gelöscht: and 250 K (-23 °C)

#### 520 4 Conclusions

521 The new high-throughput droplet freezing assay TINA was introduced to study heterogeneous  
522 ice nucleation of microliter range droplets in the immersion mode. TINA provides the analysis  
523 of 960 droplets simultaneously or 192 and 768 droplets in two independent experiments at the  
524 same time, enabling the analysis of many samples with high statistics in a short period of time.  
525 Moreover, an infrared camera-based detection system allows to reliably determine droplet  
526 freezing. The setup was tested with Snomax® as bacterial IN, and IN filtrate of *Mortierella*  
527 *alpina* as fungal IN. For these reference materials, both, the initial freezing temperature and the  
528 cumulative number of IN per gram unit mass, were in good agreement with the literature, which  
529 demonstrates the functionality of the new setup.

Gelöscht: Most of the IN active between 263 K (-10 °C) and 259 K (-14 °C) were heat-resistant. The results of both, the untreated and the heated filter extracts, showed a few outliers. These were probably caused by single large particles or aggregates larger than 5 µm, which were statistically distributed over the different dilutions. These particles nucleated at warmer subfreezing temperatures than the other IN within a dilution, so they are overestimated due to their efficient nucleation. This hypothesis is supported by the fact that the filtered filter extracts did not contain any outliers.

Gelöscht: mycelium

Gelöscht: accordance

530 TINA was applied to study the effect of O<sub>3</sub> and NO<sub>2</sub> exposure on the IN activity of  
531 Snomax®, where high concentrations of O<sub>3</sub> and NO<sub>2</sub> reduced the IN activity significantly.  
532 Atmospheric aerosol samples from Mainz (Germany) were analyzed for IN activity to show the  
533 applicability of TINA for field samples. Here, the results suggest that most of the biological IN  
534 were larger than 5 µm. Moreover, many IN active between 263 K (-10 °C) and 257 K (-16 °C)  
535 were larger than 5 µm, whereas IN active below 256 K (-17 °C) were smaller than 0.1 µm. The  
536 results confirm that TINA is suitable for high-throughput experiments and efficient analysis of  
537 biological IN in laboratory and field samples.

Gelöscht: we found highly efficient

Gelöscht: and heat-resistant IN larger than 5 µm.

557 *Author Contributions.* A.T.K., M.L., and F.H. developed the instrument. A.T.K., U.P., J.F.-N.  
558 conceived and designed the experiments. A.T.K. performed the experiments. M.L.P. wrote the  
559 code to process the data and did the error calculation. All authors discussed the data and  
560 contributed to the writing of the manuscript.

561

562 *Competing Interests.* The authors declare that they have no conflict of interest.

563

564 *Acknowledgements.* The authors thank C. Gurk, T. Klimach, F. Reubach, F. Kunz, and the  
565 workshop team for supporting the experimental setup, N. M. Kropf, C. S. Krevert, I. Maurus,  
566 G. Kopper, and P. Yordanova for technical support, and H. Grothe, T. Koop, T. Berkemeier,  
567 A. Huffman, D. A. Pickersgill, N. Lang-Yona, and J. F. Scheel for helpful discussions. The  
568 Max Planck Society (MPG) and the Ice Nuclei research Unit of the Deutsche  
569 Forschungsgemeinschaft (DFG FR 3641/1-2, FOR 1525 INUIT) are acknowledged for  
570 financial support.

571 **References**

- 572 Attard, E., Yang, H., Delort, A. M., Amato, P., Pöschl, U., Glaux, C., Koop, T. and Morris, C.  
 573 E.: Effects of atmospheric conditions on ice nucleation activity of *Pseudomonas*, *Atmos. Chem.*  
 574 *Phys.*, 12(22), 10667–10677, doi:10.5194/acp-12-10667-2012, 2012.
- 575 Ball, M. C., Wolfe, J., Canny, M., Hofmann, M., Nicotra, A. B. and Hughes, D.: Space and  
 576 time dependence of temperature and freezing in evergreen leaves, *Funct. Plant. Biol.*, 29, 1259–  
 577 1272, 2002.
- 578 Bauerecker, S., Ulbig, P., Buch, V., Vrbka, L. and Jungwirth, P.: Monitoring ice nucleation in  
 579 pure and salty water via high-speed imaging and computer simulations, *J. Phys. Chem. C*,  
 580 112(20), 7631–7636, doi:10.1021/jp711507f, 2008.
- 581 Boucher, O., Randall, D., Artaxo, P., Bretherton, C., Feingold, G., Forster, P., Kerminen, V.-  
 582 M., Kondo, Y., Liao, H., Lohmann, U., Rasch, P., Satheesh, S. K., Sherwood, S., Stevens, B.  
 583 and Zhang, X. Y.: Clouds and Aerosols, in *Climate Change 2013: The Physical Science Basis.*  
 584 Contribution of Working Group I to the Fifth Assessment Report of the Intergovernmental  
 585 Panel on Climate Change, edited by T. F. Stocker, D. Qin, G.-K. Plattner, M. Tignor, S. K.  
 586 Allen, J. Boschung, A. Nauels, Y. Xia, V. B. And, and P. M. Midgley, pp. 571–657, Cambridge  
 587 University Press, Cambridge, United Kingdom and New York, NY, USA., 2013.
- 588 Budke, C. and Koop, T.: BINARY: an optical freezing array for assessing temperature and time  
 589 dependence of heterogeneous ice nucleation, *Atmos. Meas. Tech.*, 8(2), 689–703,  
 590 doi:10.5194/amt-8-689-2015, 2015.
- 591 Carter, J., Brennan, R. and Wisniewski, M.: Low-temperature tolerance of blackcurrant flowers,  
 592 *HortScience*, 34(5), 855–859, 1999.
- 593 Ceccardi, T. L., Heath, R. L. and Ting, I. P.: Low-temperature exotherm measurement using  
 594 infrared thermography, *HortScience*, 30(1), 140–142, 1995.
- 595 Charrier, G., Nolf, M., Leitinger, G., Charra-Vaskou, K., Losso, A., Tappeiner, U., Améglio,  
 596 T. and Mayr, S.: Monitoring of Freezing Dynamics in Trees: A Simple Phase Shift Causes  
 597 Complexity, *Plant Physiol.*, 173(4), 2196–2207, doi:10.1104/pp.16.01815, 2017.
- 598 Conen, F., Morris, C. E., Leifeld, J., Yakutin, M. V. and Alewell, C.: Biological residues define  
 599 the ice nucleation properties of soil dust, *Atmos. Chem. Phys.*, 11(18), 9643–9648,  
 600 doi:10.5194/acp-11-9643-2011, 2011.
- 601 Emteborg, H., Zeleny, R., Charoud-Got, J., Martos, G., Lüddecke, J., Schellin, H. and Teipel,  
 602 K.: Infrared thermography for monitoring of freeze-drying processes: Instrumental  
 603 developments and preliminary results, *J. Pharm. Sci.*, 103(7), 2088–2097,  
 604 doi:10.1002/jps.24017, 2014.

605 Fornea, A. P., Brooks, S. D., Dooley, J. B. and Saha, A.: Heterogeneous freezing of ice on  
606 atmospheric aerosols containing ash, soot, and soil, *J. Geophys. Res. Atmos.*, 114(13), 1–12,  
607 doi:10.1029/2009JD011958, 2009.

608 Fröhlich-Nowoisky, J., Hill, T. C. J., Pummer, B. G., Yordanova, P., Franc, G. D. and Pöschl,  
609 U.: Ice nucleation activity in the widespread soil fungi *Mortierella alpina*, *Biogeosciences*, 12,  
610 1057–1071, doi:10.5194/bg-12-1057-2015, 2015.

611 Fuller, M. . and Wisniewski, M.: The use of infrared thermal imaging in the study of ice  
612 nucleation and freezing of plants, *J. Therm. Biol.*, 23(2), 81–89, doi:10.1016/S0306-  
613 4565(98)00013-8, 1998.

614 Gallego, B., Verdú, J. R., Carrascal, L. M. and Lobo, J. M.: A protocol for analysing thermal  
615 stress in insects using infrared thermography, *J. Therm. Biol.*, 56, 113–121,  
616 doi:10.1016/j.jtherbio.2015.12.006, 2016.

617 Gómez Muñoz, C. Q., García Márquez, F. P. and Sánchez Tomás, J. M.: Ice detection using  
618 thermal infrared radiometry on wind turbine blades, *Measurement*, 93, 157–163,  
619 doi:10.1016/j.measurement.2016.06.064, 2016.

620 [Green, R. L. and Warren, G. J.: Physical and functional repetition in a bacterial ice nucleation](#)  
621 [gene, \*Nature\*, 317, 645–648, doi:10.1038/317645a0, 1985.](#)

622 Hacker, J. and Neuner, G.: Ice propagation in plants visualized at the tissue level by infrared  
623 differential thermal analysis (IDTA), *Tree Physiol.*, 27(12), 1661–70,  
624 doi:10.1093/treephys/27.12.1661, 2007.

625 Hansman, R. J. and Dershowitz, A. L.: Method of and apparatus for detection of ice accretion,  
626 1994.

627 Harrison, A. D., Whale, T. F., Rutledge, R., Lamb, S., Tarn, M. D., Porter, G. C. E., Adams,  
628 M. P., McQuaid, J. B., Morris, G. J. and Murray, B. J.: An instrument for quantifying  
629 heterogeneous ice nucleation in multiwell plates using infrared emissions to detect freezing,  
630 *Atmos. Meas. Tech.*, 11, 5629–5641, doi:10.5194/amt-2018-177, 2018.

631 Hartmann, S., Augustin, S., Clauss, T., Wex, H., Santl-Temkiv, T., Voigtländer, J.,  
632 Niedermeier, D. and Stratmann, F.: Immersion freezing of ice nucleation active protein  
633 complexes, *Atmos. Chem. Phys.*, 13, 5751–5766, doi:10.5194/acpd-12-21321-2012, 2013.

634 Häusler, T., Witek, L., Felgitsch, L., Hitzenberger, R. and Grothe, H.: Freezing on a Chip - A  
635 New Approach to Determine Heterogeneous Ice Nucleation of Micrometer-Sized Water  
636 Droplets, *Atmosphere (Basel)*, 9(4), 140, doi:10.3390/atmos9040140, 2018.

637 Hill, T. C. J., Demott, P. J., Tobo, Y., Fröhlich-Nowoisky, J., Moffett, B. F., Franc, G. D. and  
638 Kreidenweis, S. M.: Sources of organic ice nucleating particles in soils, *Atmos. Chem. Phys.*,

Gelöscht: Discuss., (June), 1–22

16, 7195–7211, doi:10.5194/acp-16-7195-2016, 2016.

Kieft, T. L. and Ruscetti, T.: Characterization of Biological Ice Nuclei from a Lichen, *J. Bacteriol.*, 172(6), 3519–3523, 1990.

Kunert, A. T., Scheel, J. F., Helleis, F., Klimach, T., Pöschl, U. and Fröhlich-Nowoisky, J.: New High-Performance Droplet Freezing Assay (HP-DFA) for the Analysis of Ice Nuclei with Complex Composition, in EGU General Assembly Conference Abstracts, vol. 18, pp. EPSC2016-6293., 2016a.

Kunert, A. T., Scheel, J. F., Helleis, F., Klimach, T., Pöschl, U. and Fröhlich-Nowoisky, J.: TINA: A New High-Performance Droplet Freezing Assay for the Analysis of Ice Nuclei with Complex Composition, in 4th Workshop - Microphysics of Ice Clouds., 2016b.

Kunert, A. T., Lamneck, M., Gurk, C., Helleis, F., Klimach, T., Scheel, J. F., Pöschl, U. and Fröhlich-Nowoisky, J.: TINA, a new fully automated high-performance droplet freezing assay coupled to a customized infrared detection system, in EGU General Assembly Conference Abstracts, vol. 19, p. 13571., 2017a.

Kunert, A. T., Lamneck, M., Gurk, C., Helleis, F., Klimach, T., Scheel, J. F., Pöschl, U. and Fröhlich-Nowoisky, J.: TINA, a new fully automated high-performance droplet freezing assay coupled to a customized infrared detection system, in 5th Workshop - Microphysics of Ice Clouds., 2017b.

Kunert, A. T., Lamneck, M., Helleis, F., Scheel, J. F., Pöschl, U. and Fröhlich-Nowoisky, J.: TINA: Twin-plate ice nucleation assay with infrared detection for high-throughput droplet freezing experiments, in INUIT Final Conference and 2nd Atmospheric Ice Nucleation Conference., 2018.

Liu, F., Lakey, P., Berkemeier, T., Tong, H., Kunert, A. T., Meusel, H., Su, H., Cheng, Y., Fröhlich-Nowoisky, J., Lai, S., Weller, M. G., Shiraiwa, M., Pöschl, U. and Kampf, C. J.: Atmospheric protein chemistry influenced by anthropogenic air pollutants: nitration and oligomerization upon exposure to ozone and nitrogen dioxide, *Faraday Discuss.*, 200, 413–427, doi:10.1039/C7FD00005G, 2017.

Möhler, O., Georgakopoulos, D. G., Morris, C. E., Benz, S., Ebert, V., Hunsmann, S., Saathoff, H., Schnaiter, M. and Wagner, R.: Heterogeneous ice nucleation activity of bacteria: new laboratory experiments at simulated cloud conditions, *Biogeosciences Discuss.*, 5(2), 1445–1468, doi:10.5194/bgd-5-1445-2008, 2008.

Murray, B. J. (Ben), Broadley, S. L., Wilson, T. W., Bull, S. J., Wills, R. H., Christenson, H. K. and Murray, E. J.: Kinetics of the homogeneous freezing of water, *Phys. Chem. Chem. Phys.*, 12(35), 10380–7, doi:10.1039/c003297b, 2010.

674 O'Sullivan, D., Murray, B. J., Malkin, T. L., Whale, T. F., Umo, N. S., Atkinson, J. D., Price,  
675 H. C., Baustian, K. J., Browse, J. and Webb, M. E.: Ice nucleation by fertile soil dusts: Relative  
676 importance of mineral and biogenic components, *Atmos. Chem. Phys.*, 14(4), 1853–1867,  
677 doi:10.5194/acp-14-1853-2014, 2014.

678 Pearce, R. S. and Fuller, M. P.: Freezing of Barley Studied by Infrared Video Thermography,  
679 *Plant Physiol.*, 125(January), 227–240, 2001.

680 [Pouleur, S., Richard, C., Martin, J. G. and Antoun, H.: Ice Nucleation Activity in \*Fusarium\*](#)  
681 [acuminatum and \*Fusarium avenaceum\*, \*Appl. Environ. Microbiol.\*, 58\(9\), 2960–2964, 1992.](#)

682 Pruppacher, H. R. and Klett, J. D.: *Microphysics of Clouds and Precipitation*, 2nd ed., Springer  
683 Netherlands, Dordrecht., 1997.

684 Pummer, B. G., Budke, C., Niedermeier, D., Felgitsch, L., Kampf, C. J., Huber, R. G., Liedl,  
685 K. R., Loerting, T., Moschen, T., Schauperl, M., Tollinger, M., Morris, C. E., Wex, H., Grothe,  
686 H., Pöschl, U., Koop, T. and Fröhlich-Nowoisky, J.: Ice nucleation by water-soluble  
687 macromolecules, *Atmos. Chem. Phys.*, 15, 4077–4091, doi:10.5194/acp-15-4077-2015, 2015.

688 Sekozawa, Y., Sugaya, S. and Gemma, H.: Observations of Ice Nucleation and Propagation in  
689 Flowers of Japanese Pear (*Pyrus pyrifolia* Nakai) using Infrared Video Thermography, *J. Japan.*  
690 *Soc. Hort. Sci.*, 73(1), 1–6, doi:10.1248/cpb.37.3229, 2004.

691 Stier, J. C., Filiault, D. L., Wisniewski, M. and Palta, J. P.: Visualization of freezing progression  
692 in turfgrasses using infrared video thermography, *Crop. Sci.*, 43(1), 415–420, 2003.

693 Stopelli, E., Conen, F., Zimmermann, L., Alewell, C. and Morris, C. E.: Freezing nucleation  
694 apparatus puts new slant on study of biological ice nucleators in precipitation, *Atmos. Chem.*  
695 *Phys.*, 7, 129–134, doi:10.5194/amt-7-129-2014, 2014.

696 Tobo, Y.: An improved approach for measuring immersion freezing in large droplets over a  
697 wide temperature range, *Sci Rep*, 6(September), 32930, doi:10.1038/srep32930, 2016.

698 [Tsumuki, H. and Konno, H.: Ice Nuclei Produced by \*Fusarium\* sp. Isolated from the Gut of the](#)  
699 [Rice Stem Borer, \*Chilo suppressalis\* Walker \(Lepidoptera: Pyralidae\), \*Biosci. Biotechnol.\*](#)  
700 [Biochem., 58, 578–579, 1994.](#)

701 Turner, M. A., Arellano, F. and Kozloff, L. M.: Three separate classes of bacterial ice nucleation  
702 structures, *J. Bacteriol.*, 172(5), 2521–2526, 1990.

703 Vali, G.: Quantitative Evaluation of Experimental Results an the Heterogeneous Freezing  
704 Nucleation of Supercooled Liquids, *J. Atmos. Sci.*, 28(3), 402–409, doi:10.1175/1520-  
705 0469(1971)028<0402:QEOERA>2.0.CO;2, 1971a.

706 Vali, G.: Supercooling of Water and Nucleation of Ice (Drop Freezer), *Am. J. Phys.*, 39(10),  
707 1125, doi:10.1119/1.1976585, 1971b.

708 Ward, P. J. and DeMott, P. J.: Preliminary experimental evaluation of Snomax snow inducer,  
709 *Pseudomonas syringae*, as an artificial ice nucleus for weather modification, *J. Weather Modif.*,  
710 21(1), 9–13, 1989.

711 Whale, T. F., Murray, B. J., O’Sullivan, D., Wilson, T. W., Umo, N. S., Baustian, K. J.,  
712 Atkinson, J. D., Workneh, D. A. and Morris, G. J.: A technique for quantifying heterogeneous  
713 ice nucleation in microlitre supercooled water droplets, *Atmos. Meas. Tech.*, 8(6), 2437–2447,  
714 doi:10.5194/amt-8-2437-2015, 2015.

715 Wisniewski, M., Lindow, S. E. and Ashworth, E. N.: Observations of Ice Nucleation and  
716 Propagation in Plants Using Infrared Video Thermography, *Plant Physiol.*, 113(2), 327–334,  
717 1997.

718 Wisniewski, M., Glenn, D. M., Gusta, L. and Fuller, M. P.: Using Infrared Thermography to  
719 Study Freezing in Plants, *HortScience*, 43(6), 1648–1651, 2008.

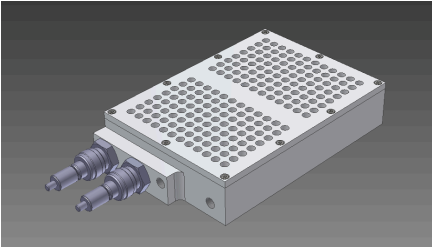
720 Workmaster, B.: Ice nucleation and propagation in cranberry uprights and fruit using infrared  
721 video thermography, *J. Amer. Soc. Hort.Sci.*, 124(6), 619–625, 1999.

722 Wright, T. P. and Petters, M. D.: The role of time in heterogeneous freezing nucleation, *J.*  
723 *Geophys. Res. Atmos.*, 118(9), 3731–3743, doi:10.1002/jgrd.503652013, 2013.

724 Zaragotas, D., Liolios, N. T. and Anastassopoulos, E.: Supercooling, ice nucleation and crystal  
725 growth: A systematic study in plant samples, *Cryobiology*, 72(3), 239–243,  
726 doi:10.1016/j.cryobiol.2016.03.012, 2016.

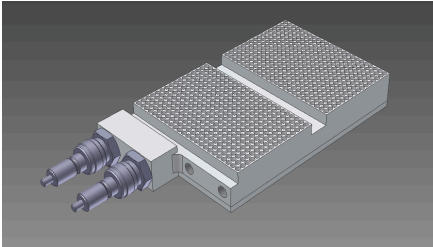
727

728 (a) 96-well sample holder block

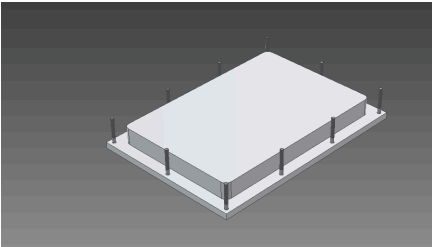


729

(d) 384-well sample holder block

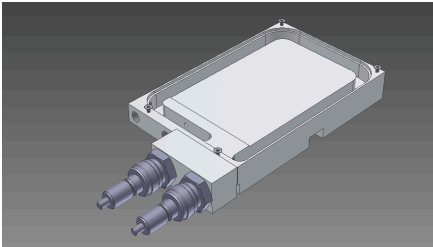


730 (b) 96-well top (flipped)

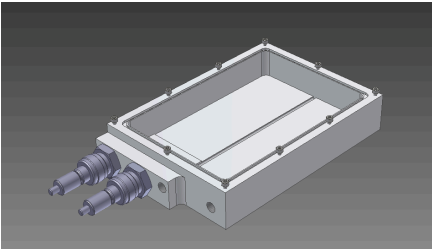


731

(e) 384-well top (flipped)

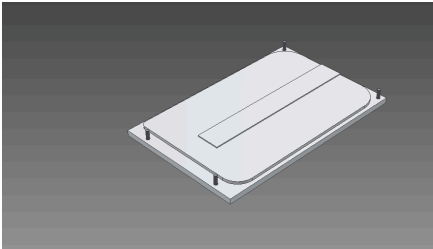


732 (c) 96-well bottom



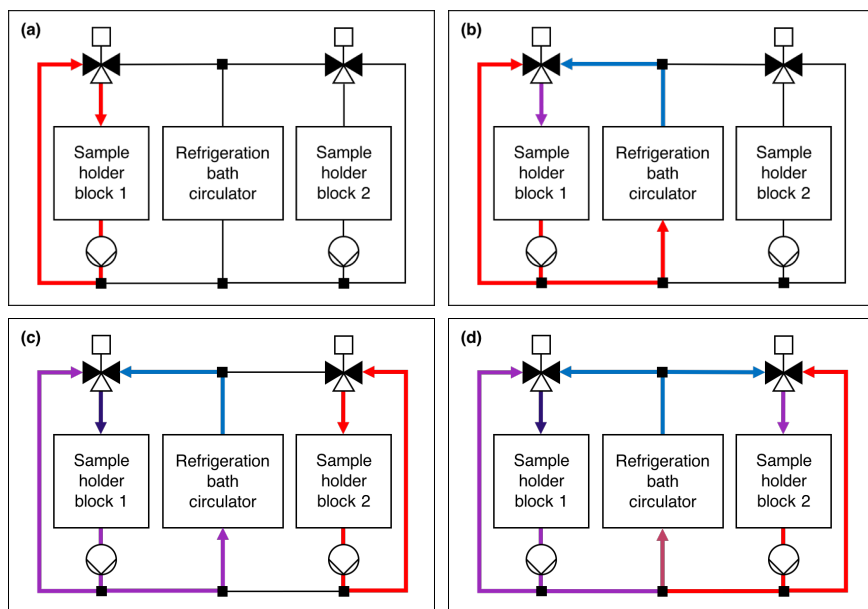
733

(f) 384-well bottom

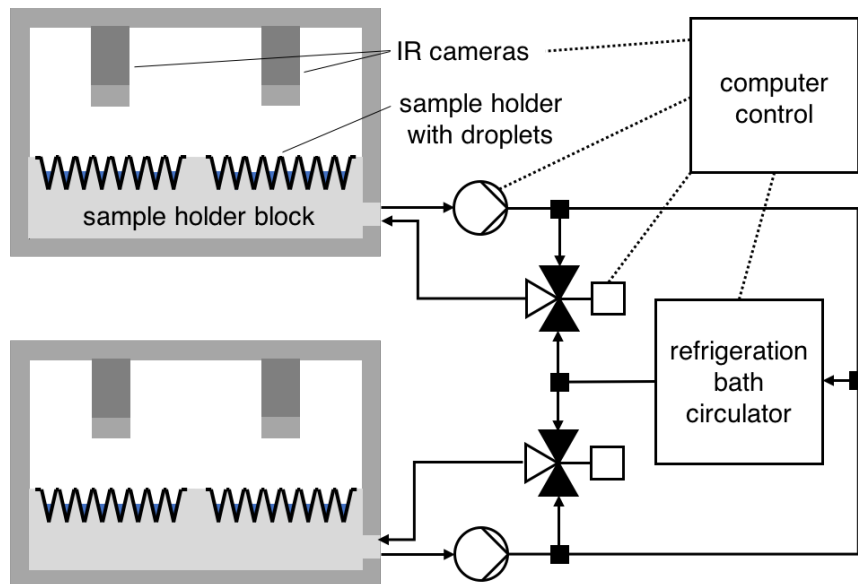


734 **Figure 1.** Sample holder and cooling blocks of the Twin-plate Ice Nucleation Assay (TINA)  
735 with (a-c) 96-well plates and (d-f) 384-well plates (CAD drawings).



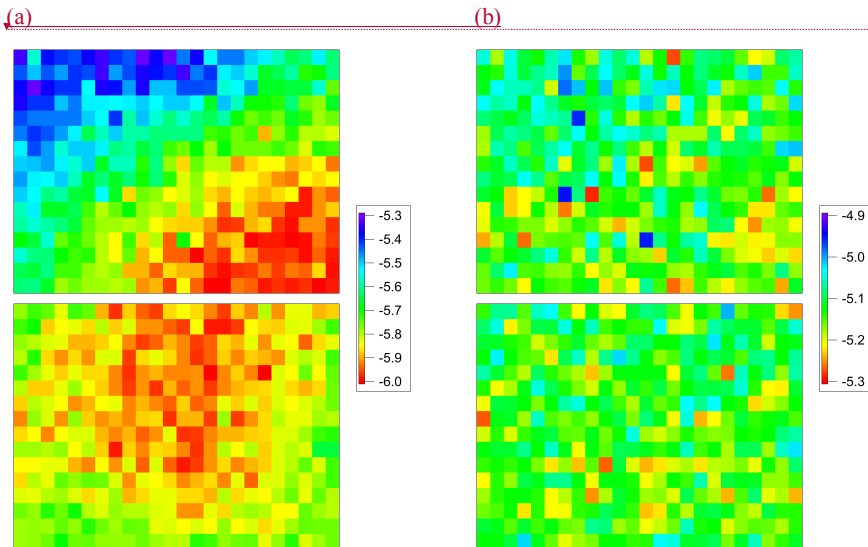


**Figure 2.** Cooling system layout and operating principle of the Twin-plate Ice Nucleation Assay (TINA). **(a)** Cooling liquid is pumped in warm cooling loop of sample holder block 1 without connection to colder cooling liquid provided by refrigeration bath circulator. **(b)** Mixing valve is opened for both, warm cooling liquid of warm cooling loop and cold cooling liquid of refrigeration bath circulator. Position of mixing valve defines temperature within sample holder block 1. **(c)** Sample holder block 1 is cooled further down, while cooling liquid is pumped in warm cooling loop of sample holder block 2. **(d)** Sample holder block 2 can be run in parallel independently from the temperature in sample holder block 1.

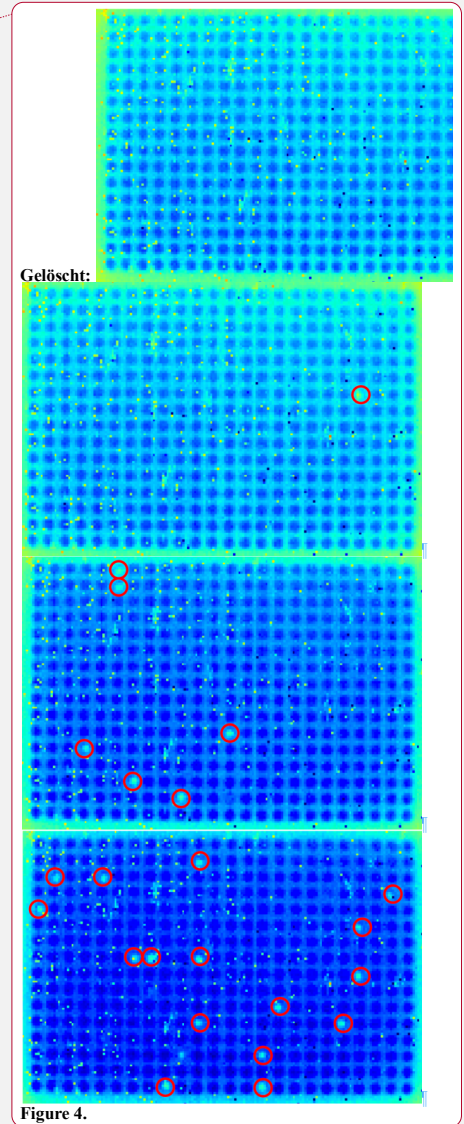


**Figure 3.** Schematic illustration of the overall setup: sample holder blocks, sample holders with droplets, IR cameras, cooling system with refrigeration bath circulator, pumps and mixing valves, computer control.

Gelöscht: 1



**Figure 4:** Measurement of temperature gradient of 384-well sample holder block using *Mortierella alpina* 13A as calibration substance. A correction matrix was calculated to compensate for temperature gradient and offset. (a) Data before correction. (b) Data after correction.



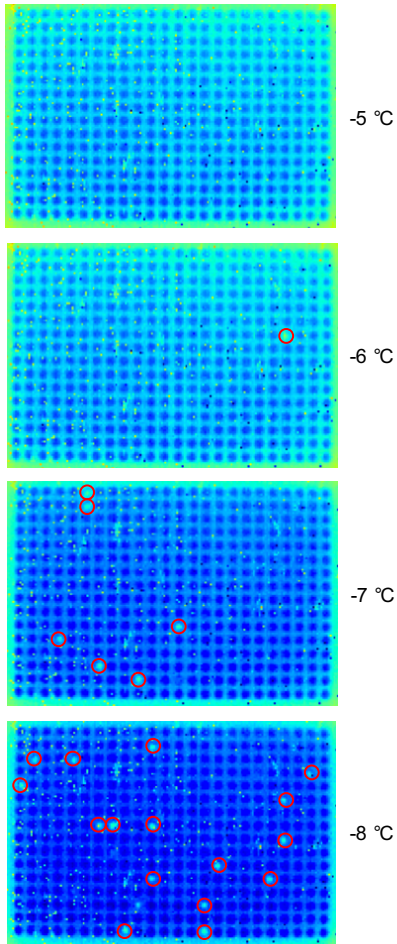


**Figure 5.** Sequence of infrared camera images showing 384 droplets during cooling. Red circles indicate freezing droplets.

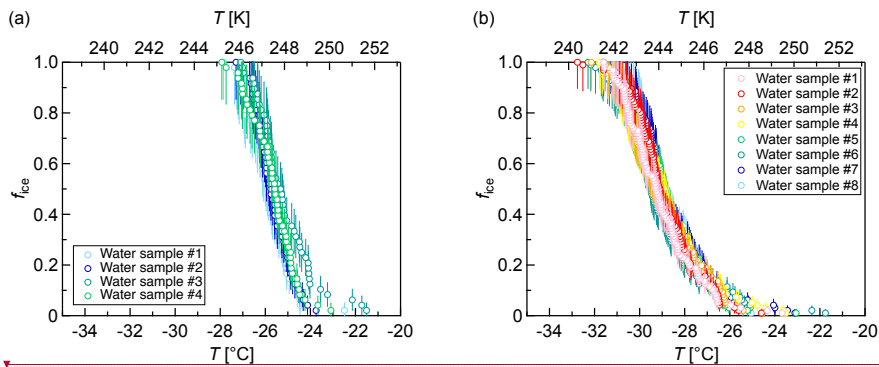
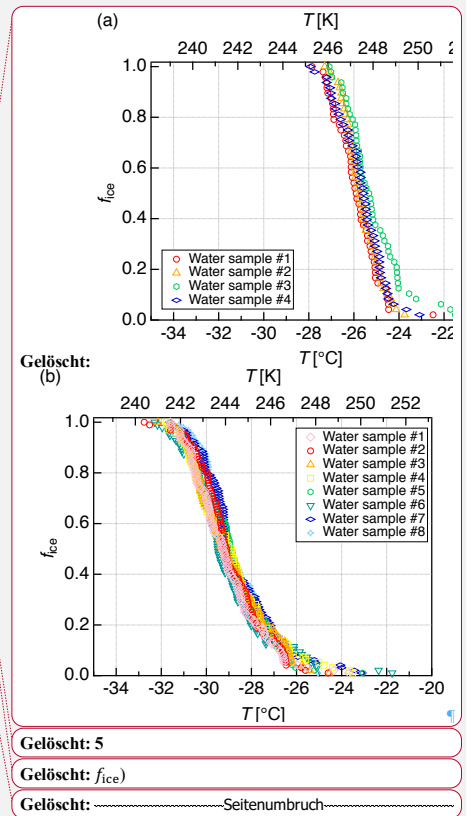


**Figure 6.** Freezing experiments with pure water droplets. Fraction of frozen droplets ( $f_{ice}$ ) vs. temperature ( $T$ ) obtained with a continuous cooling rate of  $1 \text{ K min}^{-1}$  and a droplet volume of  $3 \mu\text{L}$ . **(a)** Four different samples with 48 droplets each apportioned over two 96-well plates. **(b)** Eight different samples with 96 droplets each apportioned over two 384-well plates. The error bars were calculated using the counting error and the Gaussian error propagation. The temperature error is  $0.2 \text{ K}$ .



Gelöscht: 5

Gelöscht:  $f_{ice}$

Gelöscht: Seitenumbruch

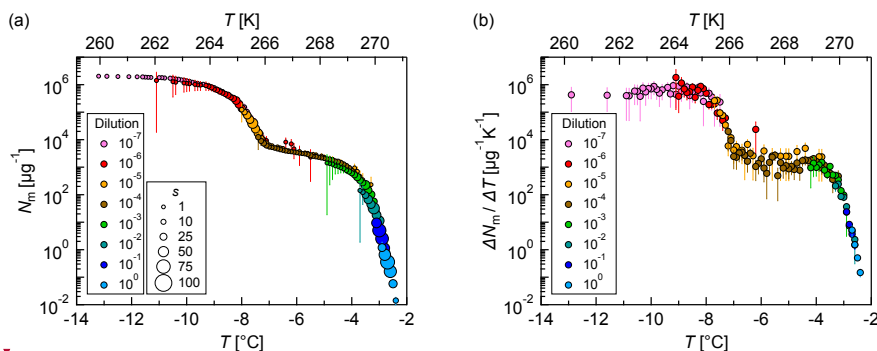


**Figure 7.** Measurements of dilution series of bacterial IN (Snomax®). (a) Cumulative number of IN ( $N_m$ ) and (b) differential number of IN ( $\Delta N_m/\Delta T$ ) per unit mass of Snomax® vs. temperature ( $T$ ). Droplets of the same dilution of three independent measurements were added to a total droplet number of 288 (3 x 96 droplets). Symbol colors indicate different dilutions; symbol size indicates the number of frozen droplets per 0.1 K bin ( $s$ ). The error bars were calculated using the counting error and the Gaussian error propagation. The temperature error is 0.2 K.

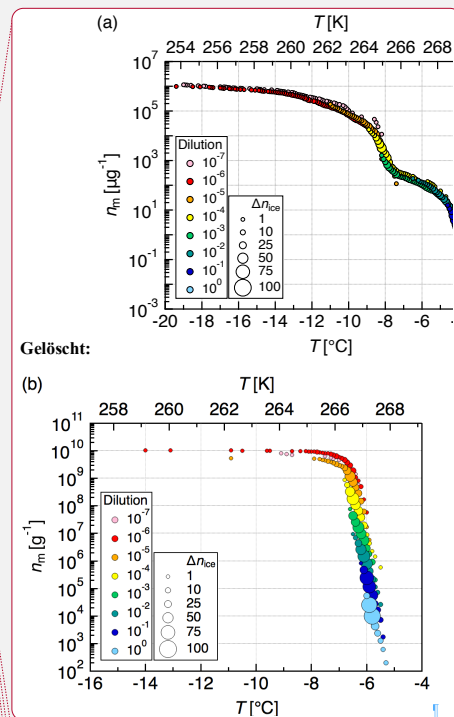


**Figure 8.** Measurements of dilution series of fungal IN (Mortierella alpina 13A). (a) Cumulative number of IN ( $N_m$ ) and (b) differential number of IN ( $\Delta N_m/\Delta T$ ) per unit mass of Mortierella alpina 13A vs. temperature ( $T$ ). Droplets of the same dilution of three independent measurements were added to a total droplet number of 288 (3 x 96 droplets). Symbol colors indicate different dilutions; symbol size indicates the number of frozen droplets per 0.1 K bin ( $s$ ). The error bars were calculated using the counting error and the Gaussian error propagation. The temperature error is 0.2 K.

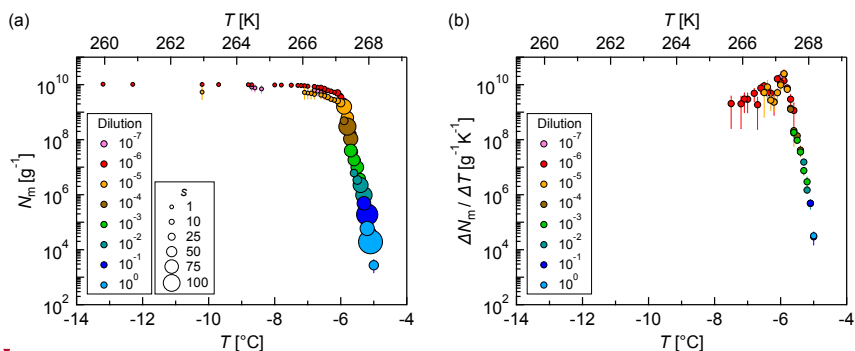


**Figure 8.** Measurements of dilution series of fungal IN (*Mortierella alpina* 13A). **(a)** Cumulative number of IN ( $N_m$ ) and **(b)** differential number of IN ( $\Delta N_m / \Delta T$ ) per unit mass of mycelium vs. temperature ( $T$ ). Droplets of the same dilution of three independent measurements were added to a total droplet number of 288 (3 x 96 droplets). Symbol colors indicate different dilutions; symbol size indicates the number of frozen droplets per 0.1 K bin ( $s$ ). The error bars were calculated using the counting error and the Gaussian error propagation. The temperature error is 0.2 K.

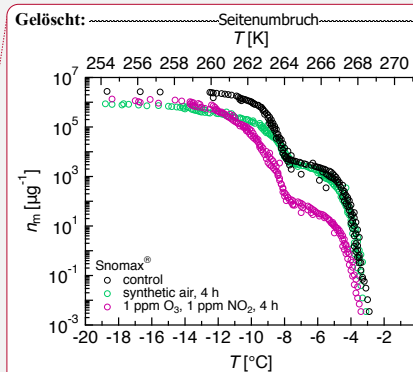


**Figure 7:**

[2] verschoben (Einfügung)

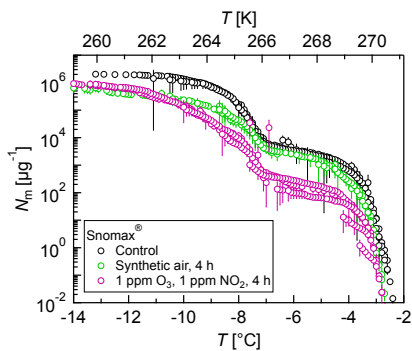


**Figure 9.** Freezing experiments with ozonized and nitrated bacterial IN. Cumulative number of IN ( $N_m$ ) per unit mass of Snomax<sup>®</sup> vs. temperature ( $T$ ). Droplets of the same dilution of three independent measurements were added to a total droplet number of 288 (3 x 96 droplets). Symbol colors indicate different exposure conditions. The error bars were calculated using the counting error and the Gaussian error propagation. The temperature error is 0.2 K.

Gelöscht:  $n_m$

Gelöscht: temperature  $T$ .

Gelöscht: —————Seitenumbruch—————



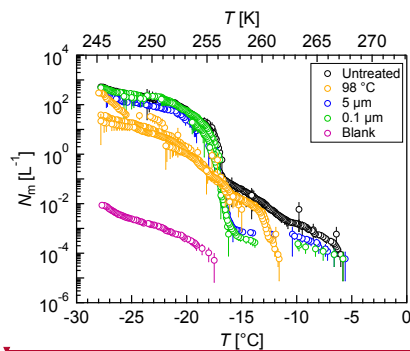
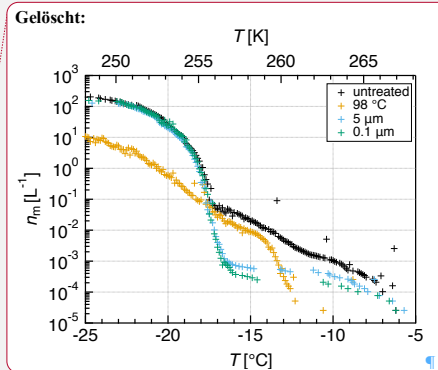


**Figure 10.** Freezing experiments with aqueous extracts of atmospheric aerosols. Cumulative number of IN per liter air ( $N_m$ ) vs. temperature ( $T$ ) for untreated (black), heated (orange), 5  $\mu\text{m}$  filtered (blue), 0.1  $\mu\text{m}$  filtered (green), and blank (purple) filter extracts. Droplets of the same dilution of two aliquots were added to a total droplet number of 192 (2 x 96 droplets). The error bars were calculated using the counting error and the Gaussian error propagation. The temperature error is 0.2 K.



[2] nach oben verschoben: Figure 8.

Gelöscht: Number

Gelöscht: and

Gelöscht: Data of different dilutions were averaged for each treatment